ALMA MATER STUDIORUM
UNIVERSITÀ DI BOLOGNA

ARCHIVIO ISTITUZIONALE
DELLA RICERCA

Alma Mater Studiorum Università di Bologna
Archivio istituzionale della ricerca

Coded Slotted ALOHA: A Graph-Based Method for Uncoordinated Multiple Access

This is the final peer-reviewed author's accepted manuscript (postprint) of the following publication:

Published Version:
Coded Slotted ALOHA: A Graph-Based Method for Uncoordinated Multiple Access / Paolini, Enrico; Liva, Gianluigi; Chiani, Marco. - In: IEEE TRANSACTIONS ON INFORMATION THEORY. - ISSN 0018-9448. - STAMPA. - 61:12(2015), pp. 7302046.6815-7302046.6832. [10.1109/TIT.2015.2492579]

Availability:
This version is available at: https://hdl.handle.net/11585/552395 since: 2016-07-14

Published:

DOI: http://doi.org/10.1109/TIT.2015.2492579

Terms of use:

Some rights reserved. The terms and conditions for the reuse of this version of the manuscript are specified in the publishing policy. For all terms of use and more information see the publisher's website.

This item was downloaded from IRIS Università di Bologna (https://cris.unibo.it/).
When citing, please refer to the published version.

(Article begins on next page)

28 April 2024

This is the final peer-reviewed accepted manuscript of:

*E. Paolini, G. Liva and M. Chiani, "**Coded Slotted ALOHA: A Graph-Based Method for Uncoordinated Multiple Access**" in IEEE Transactions on Information Theory, vol. 61, no. 12, pp. 6815-6832, Dec. 2015*

The final published version is available online at:
https://doi.org/10.1109/TIT.2015.2492579

Rights / License:

The terms and conditions for the reuse of this version of the manuscript are specified in the publishing policy. For all terms of use and more information see the publisher's website.

This item was downloaded from IRIS Università di Bologna (https://cris.unibo.it/)

When citing, please refer to the published version.

Coded Slotted ALOHA: A Graph-Based Method for Uncoordinated Multiple Access

Enrico Paolini, *Member, IEEE*, Gianluigi Liva, *Senior Member, IEEE*, and Marco Chiani, *Fellow, IEEE*

***Abstract*—In this paper, a random access scheme is introduced which relies on the combination of packet erasure correcting codes and successive interference cancellation (SIC). The scheme is named coded slotted ALOHA. A bipartite graph representation of the SIC process, resembling iterative decoding of generalized low-density parity-check codes over the erasure channel, is exploited to optimize the selection probabilities of the component erasure correcting codes via density evolution analysis. The capacity (in packets per slot) of the scheme is then analyzed in the context of the collision channel without feedback. Moreover, a capacity bound is developed and component code distributions tightly approaching the bound are derived.**

***Index Terms*—Codes on graphs, collision channel, density evolution, erasure channel, interference cancellation, iterative decoding, random access.**

I. Introduction

RANDOM multiple access has traditionally represented a popular solution for wireless networks. The slotted ALOHA protocol [1]–[4], for example, is still employed for the initial access in both cellular terrestrial and satellite communication networks [5]. As opposed to demand assignment multiple access (DAMA) protocols, random access schemes let a common channel to be dynamically and opportunistically shared by a population of users, among whom only a low level of coordination (or even no coordination at all) is permitted. In practice, the impossibility to establish a sufficient level of coordination among the users wishing to access the channel may be due to several reasons, for instance, to a lack of global information, to intolerable delays introduced by coordination establishment, to a too large user population size, or to the sporadic and unpredictable nature of users' access activity. As a result of the uncoordinated users' transmissions packets may experience *collisions*, traditionally requiring the retransmission of (some of) the involved packets, resulting in stability issues. For a random multiple access system in which each user is equipped with a buffer of infinite size to store packets that have not yet been transmitted or correctly received, stability is often intended as the property that all users' queues admit a limiting distribution (a formal definition may be found, for instance, in [6]). The *stability region* of random multiple access systems under different interacting queue settings has been deeply investigated in several works, such as [7]–[10].

A new light on random access techniques has recently been cast by the observation that iterative signal processing can largely improve the transmission efficiency, rendering the throughput achievable by random access schemes competitive with that typical of coordinated protocols. In this respect, successive interference cancellation (SIC) techniques turned out to represent a major breakthrough, enabling collisions to be favorably exploited instead of being regarded simply as a waste. These techniques share the feature of cancelling the interference caused by collided packets in the slots where they have been transmitted whenever a clean (i.e., uncollided) copy of them is detected. These advances have opened a completely new perspective in uncoordinated protocols, paving the way to dramatic performance improvements. 1

The contention resolution diversity slotted ALOHA (CRDSA) scheme proposed in [11], for example, exploits SIC in the framework of satellite access networks to remarkably improve the performance of the diversity slotted ALOHA (DSA) technique [12], consisting of transmitting each packet twice over a medium access control (MAC) frame. Almost contemporaneously to [11], interference cancellation was employed within the SICTA protocol [13] and, slightly later, within the ZigZag protocol [14]. The SICTA protocol exhibits conspicuous performance gains over collision resolution algorithms working on trees [15]. The ZigZag technique, combining packet repetitions and random packet jitters, was proposed as an effective countermeasure to collisions due to the hidden terminal problem in wireless local area networks. More recently, irregular repetition slotted ALOHA (IRSA) was introduced in [16] to provide a further throughput gain over CRDSA, by allowing a variable and judiciously designed repetition rate for each packet. (The IRSA scheme may be regarded a special case of the access technique proposed in this paper, as it will be explained later.) Moreover, an improvement to the original ZigZag approach, exploiting soft message-passing and named SigSag, was presented in [17]. Both [16] and [17] identified a key connection between the SIC process and iterative message-passing algorithms on sparse graphs.

The research leading to these results has received funding in part by the Italian Ministry of Education, Universities and Research (MIUR) under Research Projects of Significant National Interest PRIN 2011 "GRETA" and in part by the Deutscher Akademischer Austausch Dienst (DAAD) under Fellowship no. 156. The material in this paper was presented in part at the 2011 IEEE International Conference on Communications, the 2011 IEEE Global Telecommunications Conference, the 2012 IEEE First AESS European Conference on Satellite Telecommunications, and the 2012 Asilomar Conference on Signals, Systems, and Computers.

Enrico Paolini and Marco Chiani are with the Department of Electrical, Electronic, and Information Engineering "G. Marconi", University of Bologna, 47521 Cesena (FC), Italy. E-mail: {e.paolini, marco.chiani}@unibo.it

Gianluigi Liva is with Institute of Communication and Navigation of the Deutsches Zentrum fur Luft- und Raumfahrt (DLR), 82234 Wessling, Germany. E-mail: Gianluigi.Liva@dlr.de

Copyright (c) 2014 IEEE. Personal use of this material is permitted. However, permission to use this material for any other purposes must be obtained from the IEEE by sending a request to pubs-permissions@ieee.org.

This connection was exploited in [16] to design via density evolution [18] IRSA configurations with remarkably high peak throughput values, and in [17] to interpret the original ZigZag algorithm as an instance of the sum-product algorithm on factor graphs [19] and, consequently, to develop a soft version of it. Additional significant works in the area are [20], [21] in which a "frameless" version of IRSA has been proposed in analogy with rateless codes, [22] in which an IRSA configuration based on the "soliton distribution" has been developed achieving a throughput equal to $1\,[\text{packets/slot}]$, and [23] in which an unslotted version of CRDSA and IRSA was investigated. It is worth observing that SIC techniques have also been successfully exploited to enhance access protocols beyond random access. An iterative receiver for asynchronous code-division multiple access (CDMA) systems, exploiting interference cancellation, was for example proposed in [24]. Based on an exchange of extrinsic information (in a turbo-like fashion) between the interference canceller and the error correcting decoders of individual users, the decoder exhibits very good performances upon a careful design.

While in random access systems communication reliability is typically achieved via retransmissions, the problem of recovering from collisions may also be tackled from a different perspective, i.e., from a forward error correction viewpoint. A fundamental work in this research area is [25], in which the capacity region of a "collision channel without feedback" (i.e., a multiple access channel on which collisions are unavoidable while reliability cannot be ensured by retransmissions due to the lack of a feedback channel to notify successful transmissions or collisions) was analyzed and a coding scheme achieving capacity over such channel was developed. In the setting considered in [25] collisions are caused by asynchronous (either slot-aligned or unslotted) users' transmissions and the multiaccess communication strategy is based on erasure correcting codes and on assigning different periodic protocol sequences to different users, each sequence specifying the slots in which the corresponding user is allowed to access the channel. In this way, a symmetric capacity[1] equal to $1/e\,[\text{packets/slot}]$ is achieved as the number of users accessing the channel tends to infinity, both in the slotted and in the unslotted case. Although simple and effective, the approach in [25] poses some coordination challenges, especially for a large (and varying) number of users, since user protocol sequences must be jointly assigned [26], [27]. Subsequent works elaborated on the system considered in [25]. In [28] the capacity region in the slot-synchronized case was analyzed, under the more general setting in which collision are not fully destructive due, for instance, to the adoption of multiuser detection techniques [29]. Moreover, in [30] several properties of shift-invariant protocol sequences (ensuring a constant throughput to each user regardless transmissions offsets) were exposed, along with design strategies for such sequences.

In this paper an extension of the IRSA access strategy proposed in [16], dubbed coded slotted ALOHA (CSA), is proposed. As opposed to IRSA and to the above-reviewed schemes exploiting SIC in the framework of random access, in the new scheme user packets are *encoded* prior to transmission in the MAC frame, instead of being simply *repeated*. The encoding operation is performed through local component codes (all having the same dimension) randomly drawn by the users, in an uncoordinated fashion, from a set of component codes. This latter set together with the probability mass function (p.m.f.) according to which users pick their codes represent the design parameters of the proposed access scheme. On the receiver side, SIC is combined with decoding of the local component codes to recover from collisions. Exploiting a bipartite graph representation, density evolution equations for CSA on the collision channel are derived, allowing the analysis of the SIC process in an asymptotic setting and leading to the definition of the "capacity" of the scheme in a retransmission-free context. It is proved that the scheme is asymptotically reliable on the collision channel even without retransmissions. More specifically, in the limit where the MAC frame length and the user population size both tend to infinity (their ratio remaining constant), a vanishing packet loss probability is guaranteed for channel loads not greater than the asymptotic throughput.

The IRSA access scheme can be seen as an instance of CSA, where all local component codes are repetition codes. For this reason, CSA retains all advantages of IRSA in terms of uncoordinated access, equal medium access opportunities for all users, and low complexity processing performed by the users, while overcoming the main weakness of the IRSA protocol. As discussed in the next section upon addressing the system model, in fact, while the maximum *rate*[2] for an IRSA scheme able to reliably operate without retransmissions (up to some value of the load) is $1/2$, a reliable CSA scheme can be designed for any rate between 0 and 1. If, on the one hand, replacing repetition codes with generic linear block codes may appear as the simplest generalization which allows to overcome the IRSA limitation in terms of supportable rates, on the other hand this change defines a framework sufficiently general to include, as marginal variations, several other related access schemes that may be obtained by relaxing some of the conditions in the IRSA paradigm. Among them, the introduction of mild forms of coordination among the users aimed at improving the throughput, the introduction of mechanisms for making the traffic generated by some users priority with respect to the traffic generated by the other users, and the introduction of forms of inter-frame processing to resolve the collisions.

With respect to IRSA, the CSA access protocol is particularly useful in those contexts in which efficiency in terms of transmitted energy is required. In fact, the transmitted energy per packet required by CSA is higher than that required by pure slotted ALOHA by a factor that is equal to the ratio of the expected length of the component code drawn by the generic user to the (common) dimension of the component codes, i.e., a factor equal to the inverse of the rate of the scheme. Therefore, the use of local codes with low rates, as it is the case

[1]This is the maximum sum-rate for a point in the capacity region under the hypothesis that all users have the same information rate.

[2]The rate of the access scheme is formally defined in Section II-B.

for the repetition codes used in IRSA, results in low energy efficiencies, as further discussed in Section II-B. Conversely, CSA is able to overcome this limitation by admitting high-rate erasure codes as local component codes, allowing in principle rates of the access scheme arbitrarily close to 1 and thus extending the trade-off between energy efficiency and sustainable channel traffic.

In the high rate regime, i.e., for rates of the access scheme larger than $1/2$, the CSA protocol must rely on component codes with large enough dimension and high enough coding rate. In the low rate regime, i.e., for rates of the access scheme lower than $1/2$, any CSA scheme has an IRSA counterpart. Although advantages of CSA protocols over IRSA ones in terms of peak throughput transpire from our results over the whole range of low rates, these advantages are so small at very low rates (e.g., rates less than $1/3$) that IRSA protocols should be preferred in this rate region due to their design and to operational simplicity. On the contrary, when IRSA is operated at rate $1/2$ or close to it, the lack of freedom in the definition of the probability with which a component repetition code is selected results in visible performance degradation [16]. Owing to its flexibility in selecting high-rate local codes, CSA can rely on a broader set of component codes, allowing a careful definition of the probability with which each of them is picked at any target rate. As a result, for rates comprised between $1/3$ and $1/2$, CSA outperforms IRSA remarkably, even using very simple binary two-dimensional component codes.

References [31]–[34] are particularly relevant to the present work. Elaborating on some of the results developed in these works, a complete characterization and a systematic design methodology of CSA access schemes is presented and a framework for the analysis of CSA-related schemes is defined. In the process, an upper bound on the sustainable traffic for a given rate of the scheme is developed elaborating on the Area Theorem in the context of coding for erasure channels. It is illustrated in the numerical result section how, moving from CSA to IRSA, it is possible to perform closer to the bound, as previously mentioned, and that this performance advantage tends to become more evident as the dimension of the component codes increases. Moreover, an interpretation of the performance of various CSA schemes as a trade-off between energy efficiency and sustainable traffic is proposed.

In terms of possible applications, the capability of CSA to guarantee communication reliability even without retransmissions makes it an interesting opportunity for multiple access problems characterized by a potentially very large population of users (in which case the level of coordination required by DAMA protocols cannot be achieved) and in which the use of retransmissions poses some problems. Examples of such applications are wireless sensor networks with a high density of sensor nodes or radio frequency identification (RFID) systems with a high density of tags. Satellite networks are also a potential application.

This paper is organized as follows. The CSA encoding and decoding procedures, along with the adopted notation, are introduced in Section II. An asymptotic analysis of the CSA decoding process, based on an analogy with iterative decoding of modern codes on graphs, is presented in Section III, while in Section IV an upper bound on the capacity of the scheme (to be defined later) is developed. Numerical results are presented in Section V to illustrate the effectiveness of the asymptotic analysis in designing CSA configurations for a finite number of users. Conclusions follow in Section VI. Results supporting some assumptions made during the analysis and an alternative proof of the bound in Section IV are presented in the appendices.

II. CSA System Model

A. Preliminaries

We consider a slotted random access scheme where slots are grouped in MAC frames, all with the same length M (in slots). Each slot has a time duration T_{slot}, whereas the MAC frame is of time duration T_{frame}, so $M = T_{\mathsf{frame}}/T_{\mathsf{slot}}$. The total number of users in the system is $N = \alpha M$, where α is the normalized user population size.[3] Each user is frame- and slot-synchronous and attempts at most one *burst* (i.e., packet) transmission per MAC frame. Neglecting guard times, the time duration of a burst is T_{slot}.

At the beginning of a MAC frame each user generates a burst to be transmitted within the frame with probability π, where π is called the *activation probability*. Users attempting the transmission within a MAC frame are referred to as the *active* users for that frame. Since each user becomes active independently of the other users, the number of active users for a frame is modeled by a random variable N_{a} (the subscript "a" reminding the word "active") which is binomially distributed with mean value $\mathbb{E}[N_{\mathsf{a}}] = \pi N$. The instantaneous channel load is

$$G_{\mathsf{a}} = \frac{N_{\mathsf{a}}}{M} \tag{1}$$

while the expected channel load (representing the expected number of burst transmissions per slot) is

$$G = \frac{\mathbb{E}[N_{\mathsf{a}}]}{M} = \pi\alpha\,. \tag{2}$$

Clearly, for constant normalized population size α we have $G_{\mathsf{a}} = G + o(1)$ as $M \to \infty$.

B. Encoding and Decoding Procedures

The proposed access scheme works as follows. Prior to transmission, the burst of an active user is divided into k information (or data) *segments*, all of the same length in bits. The k segments are then encoded by the user via a packet-oriented linear block code generating n_h encoded segments, all of the same length as the data segments. For each transmission, the (n_h, k) code is chosen randomly by the user from a set $\mathcal{C} = \{\mathscr{C}_1, \mathscr{C}_2, \ldots, \mathscr{C}_\theta\}$ of θ *component codes*. Note that the set $\mathcal{C}$ is known also to the receiver. Unless explicitly

[3]Even if this is not mathematically necessary for the technical results presented in the following, the population size should be thought as large with respect to the number of available slots per frame, i.e., $\alpha \gg 1$. Moreover, it is useful (even if, again, not strictly necessary) to think of users characterized by a *sporadic* activity, i.e., characterized by an activation probability (defined later) $\pi \ll 1$. This justifies the use of random access schemes instead of DAMA ones.

stated, all component codes will be assumed to be binary. For $h \in \{1, 2, \ldots, \theta\}$ the code $\mathscr{C}_h$ has length n_h, dimension k, rate $R_h = k/n_h$, and minimum distance $d_h \geq 2$. Moreover, it has no idle symbols. At any transmission, each user draws its local code from the set $\mathcal{C}$ independently of all its previous choices and without any coordination with the other users. The code is picked according to a probability mass function (p.m.f.) $\mathbf{\Lambda} = \{\Lambda_h\}_{h=1}^{\theta}$ which is the same for all users. A user adopting code $\mathscr{C}_h$ for transmission in a MAC frame is referred to as a type-h user for that frame and an encoded segment associated with the user as a type-h segment. For $h \in \{1, \ldots, \theta\}$, a type-$h$ encoded segment is equipped with information about the user it is associated with and about the component code picked by the user. Moreover, it is equipped with pointers to the other $n_h - 1$ encoded segments.[4]

Encoded segments are further encoded via a physical layer code before transmission over the multiple access channel. The time duration of each transmitted segment is $T_{\mathsf{segment}} = T_{\mathsf{slot}}/k$. Every slot in the MAC frame is divided into k *slices*, each of the same time duration T_{segment} as encoded segments. Hence, up to k segments may be accommodated in the same slot and the MAC frame may be thought as composed of kM slices.[5] The n_h segments are transmitted by a type-h active user over n_h slices picked uniformly at random. We define the *rate* of the scheme as

$$R = \frac{k}{\bar{n}} \tag{3}$$

where

$$\bar{n} = \sum_{h=1}^{\theta} \Lambda_h n_h \tag{4}$$

is the expected length of the code picked in $\mathcal{C}$. Note that $\Delta E = 10 \log_{10}(\bar{n}/k) = -10 \log_{10} R$ represents the increment (in dB) of energy per burst with respect to pure SA without retransmissions. Note also that, if all component codes in the set $\mathcal{C}$ are repetition codes ($k = 1$), then the IRSA scheme is obtained as a special case of CSA. While only rates $0 < R \leq 1/2$ can be obtained with IRSA, the CSA scheme is more flexible in that all rates $0 < R < 1$ are in principle possible. In particular, to obtain a CSA scheme of rate R the minimum dimension k of the component codes is given by $\lceil R/(1-R) \rceil$.

Example 2.1: In Fig. 1 a pictorial representation of the encoding and transmission process is provided for the case of $N_{\mathsf{a}} = 3$ active users (indexed as user i, user j, and user l) and $kM = 10$ slices (indexed from 1 to 10). Each burst is split into $k = 2$ information segments. Out of the three users, user i employs a $(4, 2)$ linear block code (code $\mathscr{C}_h \in \mathcal{C}$) while user j and user l employ $(3, 2)$ linear block codes. User i performs systematic encoding of its two data segments, generating two parity segments. The four encoded segments are then transmitted into the MAC frame slices of indexes 1, 4, 7, 9. The encoded segments of users j and l (performing systematic encoding as well) are transmitted in slices of indexes 2, 4, 10 and 2, 6, 9, respectively. In the example physical layer coding is not represented.

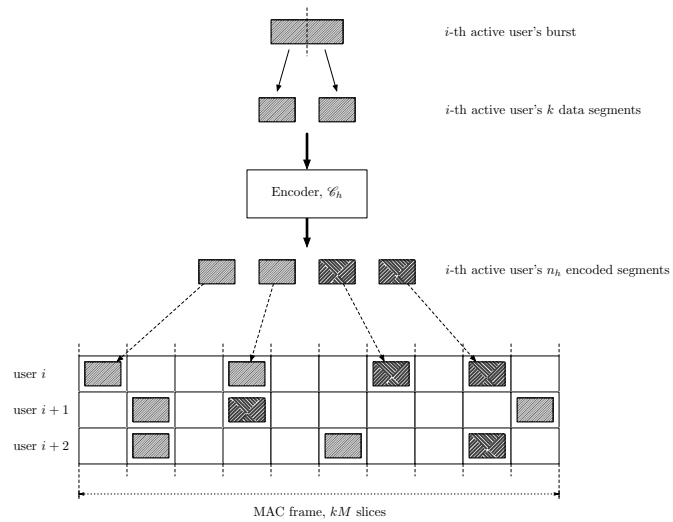

Fig. 1. Model of the CSA access scheme. Each user being active at the beginning of a MAC frame splits his bursts into $k = 2$ data segments. User i encodes his data segments via a $(4, 2)$ linear block systematic encoder, while users j and l through $(3, 2)$ linear block systematic encoders. The darkened rectangles represent parity segments generated by the encoders.

In Example 2.1 all users perform systematic encoding of their data segments. Indeed, as it will become clear in Section III, the performance of the proposed access scheme does not depend on the specific choice of the generator matrix for each code $\mathscr{C}_h \in \mathcal{C}$, so that a systematic segment encoding process may always been assumed.

On the receiver side decoding is performed as follows. Segments that are received in clean slices (i.e., segments not experiencing collisions) are first decoded at physical layer and information about the relevant user, the code $\mathscr{C}_h \in \mathcal{C}$ adopted by the user, and the positions of the other $n_h - 1$ segments in the MAC frame are extracted. For each active user the receiver becomes aware of, maximum-a-posteriori (MAP) erasure decoding of the code $\mathscr{C}_h \in \mathcal{C}$ adopted by the user is performed in order to recover as many encoded segments as possible for the user. Recovered segments may now be exploited in order to subtract their contribution of interference in those slices where collisions occurred. This procedure combining MAP erasure decoding of the codes employed by active users to encode their data segments and SIC is iterated until either all slices have been cleaned (and then all bursts have been successfully decoded) or collisions persist but no further encoded segments can be recovered via MAP erasure decoding. Note that the receiver is not a priori aware of the number of users becoming active and transmitting a burst in the current MAC frame. Note also that we have implicitly assumed that the receiver is always able to discriminate between "empty" segments and segments where users' waveforms have been received, and that collisions are

[4]In practical implementations, the overhead due to the inclusion of pointers in the segment header may be reduced by adopting more efficient techniques. For fixed k, one may include in the segment header the code index h together with a random seed, out of which it is possible to reconstruct (by a pre-defined pseudo-random number generator) the positions of the n_h segments.

[5]The definition of MAC frame as sequence of M slots is instrumental to the definition of instantaneous and expected loads G_{a} and G only. The actual minimum units that can be allocated to a segment transmission are the slices.

always detected by the receiver, even if information neither about the number of users causing the collision nor about the single colliding segments can be extracted from the waveform received in the corresponding slice. This is reasonable, for example, when the segment header comprises an integrity control field that is checked, on the decoder side, after physical layer decoding.

Example 2.2: With reference again to Fig. 1, assume that all users employ binary linear block codes. Specifically, assume that user i encodes its two data segments via a $(4, 2)$ code with generator matrix $\mathbf{G} = [1011, 0110]$, and that both user j and user l employ a $(3, 2)$ single parity-check (SPC) code. A collision is detected by the receiver on slices with indexes 2, 4, and 9, while interference-free segments are received on slices with indexes 1, 6, 7, and 10. It is easy to recognize that MAP erasure decoding of the block code employed by user i allows to recover the two missing segments of this user. The contributions of interference of these two segments can then be subtracted from the corresponding slices (of indexes 4 and 9), cleaning the segments transmitted by user j in slice 4 and by user l in slice 9, respectively. Iterating the process, MAP erasure decoding of the SPC codes employed by user j and user l allows to recover all of the segments transmitted by the two users.

C. Channel Model

When a segment of some user is recovered via MAP erasure decoding, a correct implementation of interference cancellation (i.e., cancellation of the contribution of interference of this segment in the corresponding slice) imposes the estimation of channel parameters such as the delay, the frequency offset, and the phase offset. Algorithms to efficiently perform this estimation have been discussed in [11], [16]. Nonetheless, throughout the paper we will adopt a channel model in which ideal interference cancellation is assumed. As discussed in Section III, this model has the advantage to establish a direct connection between the proposed random access scheme and iterative erasure decoding of a generalization of low-density parity-check (LDPC) codes. This bridge enables both a simple analysis of the SIC process, leading to the definition of key performance parameters such as the asymptotic threshold, and a simple yet effective access scheme design, in terms of selection of the component codes in $\mathcal{C}$ and of their p.m.f. $\mathbf{\Lambda}$.

In each slice of the MAC frame the decoder may detect a "silence" (no active user has transmitted in that segment), a signal corresponding to a unique segment, or a signal being the result of a collision. As discussed in the previous subsection, it is assumed that the decoder can always discriminate between these three events: In case a collision is detected, the observed signal provides no information to the decoder about the number and the values of colliding segments.[6] Moreover, segments not experiencing collisions are always correctly received. This is reasonable when a good physical layer channel code is used to individually encode each segment and when the signal-to-noise ratio (SNR) on the link is sufficiently high. We may better summarize our simplifying assumptions as follows.

Assumption 1: Collisions are always detected by the receiver.

Assumption 2: All users are within the range of detectability and decodability of the receiver.

Assumption 3: Interference cancellation is ideal, as so is the estimation of the channel parameters necessary to perform it.

Due to Assumption 2 when a segment experiences no collisions it is always correctly detected and decoded, and it is useful for the purposes of interference cancellation process. Moreover, when a segment is involved in a collision with other $d-1$ segments and the interference cancellation algorithm is able to cancel the contribution of interference of these $d-1$ segments, the recovered segment is correctly detected and decoded and, again, it becomes useful for the purposes of interference cancellation process.[7] Moreover, due to Assumption 3, hereafter we will use the terminology *interference subtraction* instead of interference cancellation, as it suggests perfect removal of a contribution of interference.

III. Bipartite Graph Model and Density Evolution Analysis

Considering an instantaneous population of N_{a} active users and a MAC frame of M slots, the frame status can be described by a bipartite graph, $\mathscr{G} = (B, S, E)$, consisting of a set B of N_{a} *burst nodes* (one for each active user), a set S of M *slice nodes* (one for each slice in the frame), and a set E of edges. An edge connects a burst node (BN) $b_i \in B$ to a slice node (SN) $s_j \in S$ if and only if the j-th slice has been selected by the i-th active user for transmission of a segment. Thus, BNs are associated with active users, SNs with slices in the frame, and edges with encoded segments. A BN corresponding to a type-h user is called a type-h BN. An edge incident on a type-h BN (and then corresponding to a type-h segment) is called a type-h edge. The number of edges connected to a BN or SN is the node degree. Therefore, a burst encoded via the code $\mathscr{C}_h$ is represented as a degree-n_h BN, and a slice where d segments collide as a degree-d SN.

On the receiver side, according to the channel model introduced in Section II-C segments experiencing collisions do not provide any information while segments received in clean slices are received reliably. Hence, after all active users have transmitted their encoded segments in the MAC frame, any BN may be thought as connected to "known" edges and to "unknown" ones so that some of its encoded segments are known, and the others unknown. At the generic BN (say of type h), erasure decoding of code $\mathscr{C}_h$ may allow to recover some of the unknown encoded segments. This enables to subtract the interference contribution of the newly recovered encoded segments from the symbol in the corresponding slice. If $d-1$ segments that collided in a SN of degree d

[6] This is typical of "collision channel" models. A more general setting (not addressed in this paper) is represented by a standard multipacket reception (MPR) channel model [9], in which a packet has a certain probability of being correctly received even in presence of interference from other packets transmitted in the same slot.

[7] A slightly more general channel model may be obtained by relaxing Assumption 2, as it is done in [35].

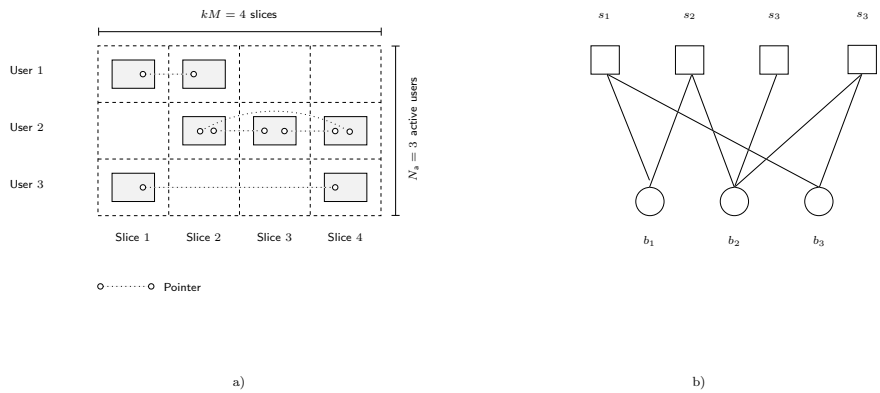

Fig. 2. On the left, a MAC frame made by $kM = 4$ slices, with $N_{\mathsf{a}} = 3$ active users. Each user is employing a repetition code. On the right, the bipartite graph representation is provided.

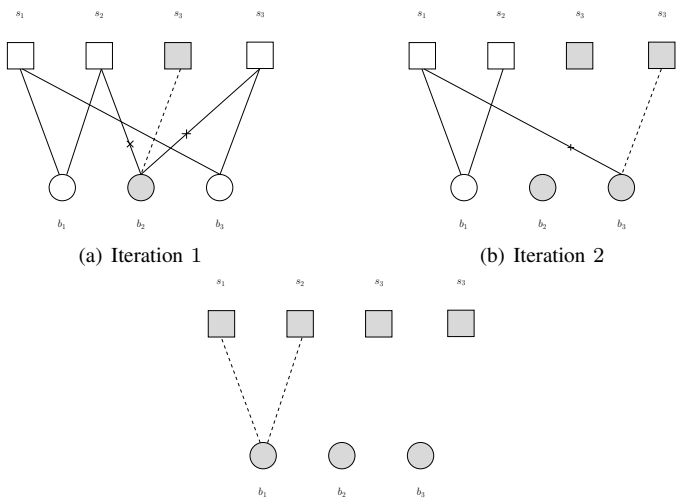

(a) Iteration 1

(b) Iteration 2

(c) Iteration 3

Fig. 3. Example of graph representation of the IIS process.

have been recovered by its neighboring BNs, the remaining segment becomes known. The interference subtraction process combined with local decoding at the BNs proceeds iteratively, i.e., cleaned slices may allow solving other collisions.

Note that this procedure is equivalent to iterative decoding of doubly-generalized low-density parity-check (D-GLDPC) codes over the erasure channel [31], where the variable nodes are generic linear block codes and the check nodes are single parity-check (SPC) codes. Then, under the assumptions stated in Section II-C the iterative interference subtraction (IIS) process admits a representation as a message-passing procedure along the edges of the above-introduced graph. Note also that the bipartite graph is not a priori known to the decoder, which "discovers" it during the iterative decoding process, based on the information available in each cleaned slice as discussed in Section II-B.

Example 3.1: In Fig. 2(a), an example of a MAC frame composed by 4 slices with $N_{\mathsf{a}} = 3$ active users is displayed. All three users adopt repetition codes ($k = 1$), thus the number of slices corresponds to the number of slots in the frame. The first and the third users encode their bursts with a $(2, 1)$ code, whereas the second user employs a $(3, 1)$ repetition code. Fig. 2(b) shows the corresponding bipartite graph model. According to the collision pattern of Fig. 2(a), the first BN is connected to the first and the second SNs, the second BN connects to the last three SNs, and the third BN is connected to the first and the fourth SNs. Fig. 3 illustrates how the graph model can be used to describe the iterative interference subtraction process. Observe the collision pattern of Fig. 2(a). The third slice contains an uncollided segment from the second user. Thus, the burst of the second user can be recovered and its interference contribution can be cancelled from the second and the fourth slice. This is shown through the graph model of Fig. 3(a), where a degree-1 SN is detected (s_3), allowing the recovery of the second burst (b_2). Following the model of Fig. 3, at the second iteration (Fig. 3(b)) a degree-1 SN is detected (s_4) allowing the recovery of the third burst (b_3). Finally, b_1 is recovered Fig. 3(c) since it is connected to two SNs and they both have degree equal to 1 in the residual graph.

A. Asymptotic Analysis of Iterative Interference Subtraction

In this subsection we analyze the evolution of the interference subtraction process in the CSA scheme, for given k and normalized population size α, in the asymptotic case where M (and correspondingly $N = \alpha M$) tends to infinity. We assume that MAP erasure decoding is performed locally at each BN.

We start by recalling the definition of information function of a linear block code [32]. Consider an (n, k) linear block code $\mathscr{C}$, where n is the codeword length and k the code dimension, and let $\mathbf{G}$ be any generator matrix of $\mathscr{C}$. Then, the g-th un-normalized information function of $\mathscr{C}$, denoted by $\tilde{e}_g$, is defined as the summation of the ranks of all possible submatrices obtained selecting g columns (with $0 \leq g \leq n$) out of $\mathbf{G}$, regardless their ordering.

Lemma 3.1: Let $M \to \infty$ for constant normalized population size α. Let $\tilde{e}_g^{(h)}$ be the g-th un-normalized information function for code $\mathscr{C}_h \in \mathcal{C}$. At the ℓ-th iteration of the SIC process, let p_ℓ be the probability that an edge is connected to a SN associated with a segment where a collision persists. Moreover, let q_ℓ be the probability that an edge is connected to

a BN whose contribution of interference on the corresponding SN cannot yet be cancelled, after MAP decoding has been performed at each BN. Then we have

$$q_\ell = \frac{1}{\bar{n}} \sum_{h=1}^{\theta} \Lambda_h \sum_{t=0}^{n_h-1} p_{\ell-1}^t (1-p_{\ell-1})^{n_h-1-t} \times \left[(n_h - t)\tilde{e}_{n_h-t}^{(h)} - (t+1)\tilde{e}_{n_h-1-t}^{(h)} \right] . \quad (5)$$

Proof: Exploiting the analogy between the IIS process and iterative decoding over the erasure channel, q_ℓ is equal to the average extrinsic erasure probability (where the average is taken over the edges of the bipartite graph) outgoing from the BNs at the ℓ-th IIS iteration. It may be computed as the extrinsic information transfer (EXIT) function of the "BN decoder" evaluated at the *a priori* erasure probability incoming from the "SN decoder", this latter probability being $p_{\ell-1}$. Denoting the EXIT function of the BN decoder under MAP decoding by $f_{\mathsf{b}}(\cdot)$, we have

$$\begin{aligned} q_\ell &= f_{\mathsf{b}}(p_{\ell-1}) \\ &= \sum_{h=1}^{\theta} \lambda_h f_{\mathsf{b}}^{(h)}(p_{\ell-1}) , \end{aligned} \quad (6)$$

where λ_h is the probability that an edge is of type h and where we have denoted by $f_{\mathsf{b}}^{(h)}(\cdot)$ the EXIT function of a type-h BN. It follows from [33] that, if the linear block code $\mathscr{C}_h$ has no idle symbols, then the function $f_{\mathsf{b}}^{(h)}(\cdot)$ may be expressed as

$$f_{\mathsf{b}}^{(h)}(p_{\ell-1}) = \frac{1}{n_h} \sum_{t=0}^{n_h-1} p_{\ell-1}^t (1-p_{\ell-1})^{n_h-1-t} \times \left[(n_h - t)\tilde{e}_{n_h-t}^{(h)} - (t+1)\tilde{e}_{n_h-1-t}^{(h)} \right] . \quad (7)$$

The theorem statement follows by incorporating (7) into (6) and by noting that $\lambda_h = \frac{\Lambda_h n_h}{\bar{n}}$. ■

Equation (5) allows to update q_ℓ given $p_{\ell-1}$. The dependence of p_ℓ on q_ℓ is instead stated by the following lemma.

Lemma 3.2: Let $M \to \infty$ for constant normalized population size α. Let R be the rate of the scheme as defined in (3). At the ℓ-th iteration of the SIC process, let p_ℓ and q_ℓ be defined as in the statement of Lemma 3.1. Then we have

$$p_\ell = 1 - \exp\left\{ -\frac{\pi\alpha}{R} q_\ell \right\} . \quad (8)$$

Proof: For $0 \le l \le M$, the probability Ψ_l to receive l encoded slices in a segment of the MAC frame is given by

$$\Psi_l = \binom{M}{l} \left(\frac{\bar{n}\pi\alpha}{kM} \right)^l \left(1 - \frac{\bar{n}\pi\alpha}{kM} \right)^{M-l} .$$

Defining $\Psi(x) = \sum_{l=0}^{M} \Psi_l x^l$ and letting $M \to \infty$ for constant α, yields

$$\Psi(x) = \exp\left\{ -\frac{\pi\alpha}{R}(1-x) \right\} . \quad (9)$$

Next, define the polynomial $\rho(x) = \sum_{l \ge 1} \rho_l x^{l-1}$, where ρ_l is the probability that an edge in the bipartite graph is connected to a SN of degree l. Note that $\rho(x)$ is equivalent to the edge oriented degree distribution polynomial for the check nodes of an ordinary LDPC code. We then have

$$\begin{aligned} \rho(x) &= \frac{1}{\Psi'(1)} \frac{\mathrm{d}\Psi(x)}{\mathrm{d}x} \\ &= \Psi(x) \end{aligned} \quad (10)$$

and, from standard density evolution of LDPC codes over the memoryless erasure channel,

$$p_\ell = 1 - \rho(1 - q_\ell)$$

which leads to (8). ■

The right-hand side of (8) represents the EXIT function of the SN decoder. Hereafter, this function will be denoted by $f_{\mathsf{s}}(\cdot)$, so

$$f_{\mathsf{s}}(q) = 1 - \exp\left\{ -\frac{\pi\alpha}{R} q \right\} . \quad (11)$$

From Lemma 3.1 and Lemma 3.2 we finally obtain a density evolution recursion for the IIS process only involving the probability p_ℓ.

Theorem 3.1 (Density evolution recursion for CSA): Let $M \to \infty$ for constant normalized population size α. Let R be the rate of the scheme as defined in (3) and $\tilde{e}_g^{(h)}$ be the g-th un-normalized information function for code $\mathscr{C}_h \in \mathcal{C}$. At the ℓ-th iteration of the SIC process, let p_ℓ be defined as in the statement of Lemma 3.1. Then we have

$$p_\ell = 1 - \exp\left\{ -\frac{\pi\alpha}{k} \sum_{h=1}^{\theta} \Lambda_h \sum_{t=0}^{n_h-1} p_{\ell-1}^t (1-p_{\ell-1})^{n_h-1-t} \times \left[(n_h - t)\tilde{e}_{n_h-t}^{(h)} - (t+1)\tilde{e}_{n_h-1-t}^{(h)} \right] \right\} \quad (12)$$

with starting point $p_0 = 1 - \exp\{-\pi\alpha/R\}$.

Proof: The recursion (12) can be easily obtained as $p_\ell = (f_{\mathsf{s}} \circ f_{\mathsf{b}})(p_{\ell-1})$, where $f_{\mathsf{b}}(\cdot)$ and $f_{\mathsf{s}}(\cdot)$ are defined in (6) and (11), respectively, also noting that from (3) we have $R\bar{n} = k$. The starting point of the recursion is equal to $p_0 = f_{\mathsf{s}}(1)$, i.e., to the average extrinsic erasure probability outgoing from the SN decoder, when no *a priori* information is available from the BN decoder. ■

The density evolution recursion (12) captures both the iterative cancellation of interference at the SNs and local MAP decoding at the BNs. It may be specialized in the IRSA case, in which all component codes in $\mathcal{C}$ are repetition codes. This is expressed by the following corollary, in which we use the convention that the h-th component code is a length-h repetition code (hence $n_h = h$) and that $\Lambda_1 = 0$.

Corollary 3.1 (Density evolution recursion for IRSA): Let $M \to \infty$ for constant normalized population size α. Let R be the rate of the scheme as defined in (3) and assume that code $\mathscr{C}_h \in \mathcal{C}$ is a length-h repetition code, for $h \in \{2, \ldots, \theta\}$. At the ℓ-th iteration of the interference subtraction process, let p_ℓ be defined as in the statement of Lemma 3.1. Then we have

$$p_\ell = 1 - \exp\left\{ -\pi\alpha \sum_{h=2}^{\theta} h\, \Lambda_h\, p_{\ell-1}^{h-1} \right\} \quad (13)$$

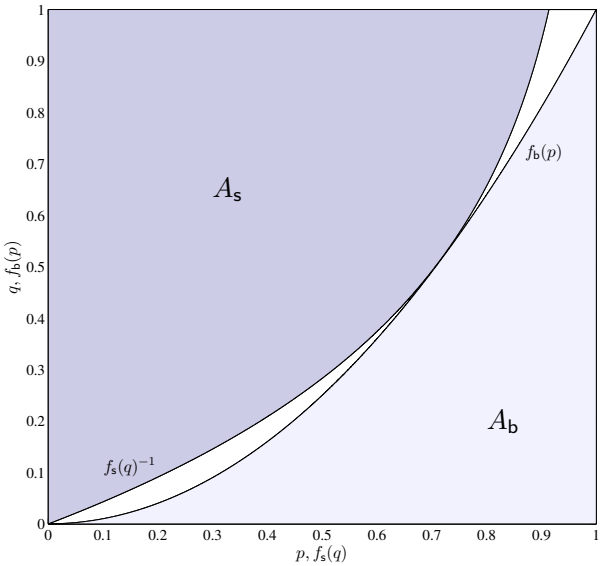

Fig. 4. EXIT chart for a regular coded random access scheme employing a rate-$1/3$ repetition code at each BN, characterized by $G^* = 0.816$.

with starting point $p_0 = 1 - \exp\{-\pi\alpha/R\}$.

Proof: The recursion (13) follows directly from (12) by observing that, when the code $\mathcal{C}_h$ is a length-h repetition code, $k = 1$ and the quantity $[(n_h - t)\tilde{e}^{(h)}_{n_h-t} - (t+1)\tilde{e}^{(h)}_{n_h-1-t}]$ is equal to zero for all $0 \le t < h-1$ and is equal to h for $t = h-1$. ■

For a given set $\mathcal{C}$ of component codes, a given p.m.f. $\mathbf{\Lambda}$ on $\mathcal{C}$, and a given normalized population size α, the *asymptotic threshold* of the CSA access scheme, denoted by $\pi^* = \pi^*(\mathcal{C}, \mathbf{\Lambda}, \alpha)$, is defined as

$$\pi^*(\mathcal{C}, \mathbf{\Lambda}, \alpha) := \sup\{\pi \ge 0 \,|\, p_\ell \to 0 \text{ as } \ell \to \infty\}$$

according to the recursion (12). The asymptotic threshold may also be defined in terms of the expected channel load, as $G^*(\mathcal{C}, \mathbf{\Lambda}) := \alpha\,\pi^*(\mathcal{C}, \mathbf{\Lambda}, \alpha)$, this latter definition having the advantage to be independent of the normalized population size. In the asymptotic setting $M \to \infty$, for all $G < G^*(\mathcal{C}, \mathbf{\Lambda})$ the throughput is $S = G$, i.e., all collisions are resolved even if packet retransmissions are forbidden. In this sense, $G^*(\mathcal{C}, \mathbf{\Lambda})$ represents the *capacity* of the CSA scheme on a slot-aligned collision channel without feedback conditional to the specific choice of $\mathcal{C} = \{\mathscr{C}_1, \mathscr{C}_2, \ldots, \mathscr{C}_\theta\}$ and $\mathbf{\Lambda}$.

The recursion defined by (5) and (8) can be visualized in an EXIT chart, which displays $f_{\mathsf{b}}(p)$ vs. $f_{\mathsf{s}}^{-1}(p)$. An example of EXIT chart for an IRSA scheme in which $\mathcal{C} = \{\mathscr{C}_1\}$ where $\mathscr{C}_1$ is $(3,1)$ repetition code is provided in Fig. 4. As the iteration index ℓ increases, the evolution of the pair of probabilities (p_ℓ, q_ℓ) traces a zig-zag pattern inside the tunnel between the two curves. Whenever we operate the scheme below its capacity, $G < G^*(\mathcal{C}, \mathbf{\Lambda})$, the two curves do not intersect, leaving the tunnel open. This lets the pair of probabilities (p_ℓ, q_ℓ) get arbitrarily close to the $(0,0)$ point. On the contrary, if the scheme is operated above its capacity, $G > G^*(\mathcal{C}, \mathbf{\Lambda})$, the two curves intersect (closing the tunnel) in a point $(\hat{p}, \hat{q})$ with $\hat{p} > 0, \hat{q} > 0$, and the IIS process converges to a fixed point corresponding to a non-zero residual erasure probability. As it was pointed out right after Example 2.1 in Section II-B, the performance of the CSA scheme does not depend on the specific choice of the generator matrices for the θ component codes. Note, in fact, that the information functions $\tilde{e}^{(h)}_g$ in (12) are independent of the representation of code $\mathscr{C}_h$, $h \in \{1, \ldots, \theta\}$, hence so are the EXIT functions and the threshold $\pi^*(\mathcal{C}, \mathbf{\Lambda}, \alpha)$. The same holds for the performance of finite-length CSA schemes, addressed in Section V.

B. Stability of Iterative Interference Subtraction Collision-Free Point

Autonomous difference equations such as (12) are often analyzed as regard to the stability of their solutions or, as a particular case, of their fixed (steady-state equilibrium) points. In this subsection we study the stability of the fixed point $\hat{p} = 0$ of (12), representing the collision-free state. We remark that stability is here intended as *convergence*, i.e., as the property of an equilibrium point $\hat{x}$ of a recursion $x_\ell = F(x_{\ell-1})$ to attract (in the sense of convergence as $\ell \to \infty$) the state x_ℓ when the initial state x_0 is perturbed from $\hat{x}$. Under this acceptation, a solution $x_\ell = \hat{x}\ \forall \ell \ge 0$ of the difference equation $x_\ell = F(x_{\ell-1})$ is said to be locally stable if there exists $\delta > 0$ such that $|x_0 - \hat{x}| < \delta$ implies $|x_\ell - \hat{x}| \to 0$ as $\ell \to \infty$. The following well-known result establishes a necessary and sufficient condition for local stability.

Lemma 3.3: A solution $x_\ell = \hat{x}\ \forall \ell \ge 0$ of a difference equation $x_\ell = F(x_{\ell-1})$, where $F : \mathbb{R} \mapsto \mathbb{R}$ is a differentiable function, is locally stable if and only if $|F'(\hat{x})| < 1$.

The application of Lemma 3.3 to (12) yields the following result.

Theorem 3.2 (Stability condition for CSA): For $h \in \{1, \ldots, \theta\}$, let $\mathscr{C}_h$ be the (n_h, k) linear block code with minimum distance $d_h \ge 2$ and without idle symbols, employed with probability Λ_h by the generic user to generate its encoded segments. Let $B^{(h)}_w$ be the number of weight-w codewords of $\mathscr{C}_h$. Moreover, let

$$r = \min_{h \in \{1,\ldots,\theta\}} \{d_h\}$$

and

$$\mathcal{H} = \{h : d_h = r\}\,.$$

If $r = 2$, then the solution $p_\ell = \hat{p} = 0\ \forall \ell \ge 0$ of recursion (12) is locally stable if and only if

$$\pi < \frac{k}{2\alpha\mathcal{B}_2} \tag{14}$$

where $\mathcal{B}_2 = \sum_{h \in \mathcal{H}} \Lambda_h B^{(h)}_2$ is the expected number of weight-2 codewords in a code picked from $\mathcal{C}$. Else, if $r \ge 3$, the fixed point $\hat{p} = 0$ of (12) is stable for any value of G.

Proof: Let us denote by $\mathbf{G}^{(h)}_g$ the generic $k \times g$ matrix obtained by selecting g columns in (any representation of) the generator matrix of code $\mathscr{C}_h$, irrespective of the order of the g columns, and by $\sum_{\mathbf{G}^{(h)}_g}$ the summation over all $\binom{n}{g}$ such matrices. Moreover, let us define

$$a^{(h)}_t := (n_h - t)\tilde{e}^{(h)}_{n_h-t} - (t+1)\tilde{e}^{(h)}_{n_h-1-t}\,.$$

We have:

$$
\begin{aligned}
&(f_{\mathsf{s}} \circ f_{\mathsf{b}})'(0) \\
&= \frac{\pi\alpha}{k} \sum_{h=1}^{\theta} \Lambda_h e^{-\frac{G\, a_0^{(h)}}{k}} \left[a_1^{(h)} - (n_h - 1) a_0^{(h)} \right] \\
&\overset{\text{(a)}}{=} \frac{\pi\alpha}{k} \sum_{h=1}^{\theta} \Lambda_h a_1^{(h)} \\
&= \frac{2\pi\alpha}{k} \sum_{h=1}^{\theta} \Lambda_h \left[\frac{(n_h - 1)\tilde{e}_{n_h-1}^{(h)}}{2} - \tilde{e}_{n_h-2}^{(h)} \right] \\
&\overset{\text{(b)}}{=} \frac{2\pi\alpha}{k} \sum_{h=1}^{\theta} \Lambda_h \left[k \binom{n_h}{n_h - 2} - \tilde{e}_{n_h-2}^{(h)} \right] \\
&= \frac{2\pi\alpha}{k} \sum_{h=1}^{\theta} \Lambda_h \sum_{\mathbf{G}_{n_h-2}^{(h)}} \left(k - \operatorname{rank}(\mathbf{G}_{n_h-2}^{(h)}) \right) \\
&\overset{\text{(c)}}{=} \begin{cases} \frac{2\pi\alpha}{k} \mathcal{B}_2 & \text{if} \quad r = 2 \\ 0 & \text{if} \quad r \geq 3 \end{cases}
\end{aligned} \tag{15}
$$

In the previous equation list (a) and (b) follow from the hypothesis $r \geq 2$. In particular, (a) is due to $a_0^{(h)} = n_h \tilde{e}_{n_h} - \tilde{e}_{n_h-1} = n_h\, k - n_h\, k = 0$ and (b) to $\tilde{e}_{n_h-1}^{(h)} = k\, n_h$, both relying on $r \geq 2$. Moreover, (c) is due to $r \geq 2$ and to [34, Proposition 2]. Inequality (14) now follows from $|(f_{\mathsf{s}} \circ f_{\mathsf{b}})'(0)| < 1$. ■

The stability condition is a necessary, but in general not sufficient condition for successful decoding in that, for given $\mathcal{C}$ and $\mathbf{\Lambda}$, values of the channel load may exist, fulfilling the bound (14) but which are above the CSA capacity. This implies

$$
G^*(\mathcal{C}, \mathbf{\Lambda}) \leq \frac{k}{2\mathcal{B}_2} \tag{16}
$$

which will be referred to as the *stability upper bound* and whose right-hand side will be denoted by $G^*_{\mathsf{sb}}(\mathcal{C}, \mathbf{\Lambda})$. Note that in the IRSA case ($k = 1$) we have $\mathcal{B}_2 = \Lambda_2$, where Λ_2 is the probability to select the length-2 repetition code from the set $\mathcal{C}$, which yields[8]

$$
G^*(\mathcal{C}, \mathbf{\Lambda}) \leq \frac{1}{2\Lambda_2}\,.
$$

When $r = 2$, (16) may be achieved with equality, this situation being equivalent to the well-known *flatness condition* for LDPC codes [36]. This is the case, for example, when $\theta = 1$ and the binary linear block code employed by all users is a $(k+1, k)$ SPC code, as stated by the following corollary.

Corollary 3.2: Let $\mathcal{C} = \{\mathscr{C}\}$ and the linear block code $\mathscr{C}$ employed by all users be a $(k+1, k)$ SPC code. Then

$$
G^*(\mathcal{C}, \mathbf{\Lambda}) = \frac{1}{k+1}\,. \tag{17}
$$

Proof: If all users employ a $(k+1, k)$ SPC code, then the stability bound (16) becomes $G^*(\mathcal{C}, \mathbf{\Lambda}) \leq 1/(k+1)$. In order to prove that the bound is achieved with equality, it suffices to show that density evolution recursion (12), which assumes the simple form[9]

$$
p_\ell = 1 - \exp\left\{ -\frac{(k+1)\pi\alpha}{k} \left[1 - (1 - p_{\ell-1})^k \right] \right\}, \tag{18}
$$

converges to 0 as $\ell \to \infty$ for $\pi\alpha = 1/(k+1)$. The result follows by observing that the function

$$
F(p) = 1 - \exp\left\{ -\frac{1}{k} [1 - (1-p)^k] \right\}
$$

fulfills $F'(0) = 1$ (hence its graph is tangent to that of the function $I(p) = p$ in the $(0, 0)$ point), $F'(p) = \exp\{-\frac{1}{k}[1 - (1-p)^k]\}(1-p)^{k-1} > 0$ for all $p \in [0, 1)$, and $F''(p) = -\exp\{-\frac{1}{k}[1-(1-p)^k]\}[(1-p)^{2k-2} + (k-1)(1-p)^{k-2}] < 0$ for all $p \in [0, 1)$. ■

C. Asymptotic Analysis Under a Random Component Code Hypothesis

In the system model description provided in Section II, the generic user has been assumed to encode its k information segments via an (n_h, k) binary linear block code, with minimum distance $d_h \geq 2$, picked randomly with p.m.f. $\mathbf{\Lambda} = \{\Lambda_h\}_{h=1}^{\theta}$ from an ensemble of θ component codes. In this subsection, we consider a slightly different setting. Specifically, we assume that the generic user randomly picks a codeword length $n_s > k$ from an ensemble $\mathscr{N} = \{n_1, \ldots, n_{s_{\max}}\}$ with p.m.f. $\mathbf{\Lambda} = \{\Lambda_{n_s}\}_{s=1}^{s_{\max}}$ and encodes its k segments through a binary $k \times n_s$ generator matrix drawn randomly with uniform probability from the set of all $k \times n_s$ binary matrices with rank k and representing (n_s, k) linear block codes without idle bits and with minimum distance at least 2. We are interested in calculating the expected asymptotic threshold for this scheme, where expectation is over all such generator matrices. The advantage of this *random code hypothesis* is that it allows to release the analysis from considering a specific set of θ codes.

With respect to the previous case, the definition (3) of the rate R and the expressions (9) and (10) of $\Psi(x)$ and $\rho(x)$, respectively, remain unchanged provided the definition of $\bar{n}$ is updated as $\bar{n} = \sum_{s=1}^{s_{\max}} \Lambda_{n_s} n_s$. Analogously, the recursion (8) is not affected by the random code hypothesis. On the other hand, the recursion (5) is updated as follows. Denote by $\mathsf{G}_{n_s,k}$ the ensemble of all $k \times n_s$ binary matrices with rank k representing linear block codes without idle bits and with minimum distance at least 2, and by $\mathbb{E}_{\mathsf{G}_{n_s,k}}[\cdot]$ the expectation operator over the set $\mathsf{G}_{n_s,k}$ (with a uniform probability measure). Then we have

$$
\begin{aligned}
q_\ell = &\frac{1}{\bar{n}} \sum_{s=1}^{s_{\max}} \Lambda_{n_s} \sum_{t=0}^{n_s-1} p_{\ell-1}^t (1 - p_{\ell-1})^{n_s-1-t} \\
&\times \left[(n_s - t) \mathbb{E}_{\mathsf{G}_{n_s,k}} \left[\tilde{e}_{n_s-t} \right] - (t+1) \mathbb{E}_{\mathsf{G}_{n_s,k}} \left[\tilde{e}_{n_s-1-t} \right] \right]
\end{aligned} \tag{19}
$$

[8]The stability condition for the IRSA scheme appears in [16, Eq. (7)].

[9]This form follows from the duality property proved in [33, Section IV-E].

where again $\bar{n} = \sum_{s=1}^{s_{\max}} \Lambda_{n_s} n_s$. For $0 < k < n_s$ and $0 \leq g \leq n_s$, the expected g-th unnormalized information $\mathbb{E}_{\mathsf{G}_{n_s,k}}[\tilde{e}_g]$ may be calculated using results from [31], in particular as

$$\mathbb{E}_{\mathsf{G}_{n_s,k}}[\tilde{e}_g] = \binom{n_s}{g} \sum_{u=1}^{\min\{k,g\}} u \, \frac{K(k,n_s,g,u,k)}{J(k,n_s,k)} \tag{20}$$

where $J(k,n_s,k)$ denotes the number of $k \times n_s$ binary matrices with rank k, without all-zero columns and without independent columns,[10] and where $K(k,n_s,g,u,k)$ is the number of $k \times n_s$ binary matrices with rank k, without all-zero columns, without independent columns and such that their left-most g columns have rank u. The functions $J(m,n,r)$ and $K(m,n,g,u,r)$ may be evaluated recursively, as detailed in [31, Theorem 4] and [31, Theorem 5], respectively.

Density evolution recursion for CSA under the random code hypothesis is then given by

$$p_\ell = 1 - \exp\Bigg\{ -\frac{\pi\alpha}{k} \sum_{s=1}^{n_s} \Lambda_{n_s} \sum_{t=0}^{n_s-1} p_{\ell-1}^t (1-p_{\ell-1})^{n_s-1-t} \times \left[(n_s-t)\mathbb{E}_{\mathsf{G}_{n_s,k}}[\tilde{e}_{n_s-t}] - (t+1)\mathbb{E}_{\mathsf{G}_{n_s,k}}[\tilde{e}_{n_s-1-t}] \right] \Bigg\} \tag{21}$$

with starting point $p_0 = 1 - \exp\{-\pi\alpha/R\}$. For given $\mathscr{N} = \{n_1, \ldots, n_{s_{\max}}\}$ and $\mathbf{\Lambda} = \{\Lambda_{n_s}\}_{s=1}^{s_{\max}}$, the expected asymptotic threshold of the CSA scheme under the random code hypothesis, denoted by $G^* = G^*(\mathscr{N}, \mathbf{\Lambda})$, is defined as the supremum of the ensemble of all $G \geq 0$ such that $p_\ell \to 0$ as $\ell \to \infty$ in recursion (21).

Using a proof technique analogous to that of Theorem 3.2, it is easy to show that the stability upper bound is again given by (16), where now $\mathcal{B}_2 = \sum_{s=1}^{s_{\max}} \Lambda_{n_s} \mathbb{E}_{\mathsf{G}_{n_s,k}}[B_2]$ and

$$\mathbb{E}_{\mathsf{G}_{n_s,k}}[B_2] = \binom{n_s}{2} \left(k - \sum_{u=1}^{\min\{k,n_s-2\}} u \, \frac{K(k,n_s,n_s-2,u,k)}{J(k,n_s,k)} \right)$$

is the expected number of weight-2 codewords of an (n_s,k) linear block code whose generator matrix is picked uniformly at random in the set $\mathsf{G}_{n_s,k}$.

IV. Capacity Limits of CSA Schemes

In this section, we develop an upper bound on the capacity of the CSA scheme, for a given rate R. The upper bound is established in the following theorem.

Theorem 4.1: For $0 < R \leq 1$, let $\mathbb{G}(R)$ be the unique positive solution of the equation

$$G = 1 - e^{-G/R} \tag{22}$$

in $[0,1)$. Then, the capacity $G^*(\mathcal{C}, \mathbf{\Lambda})$ of the CSA scheme fulfills

$$G^*(\mathcal{C}, \mathbf{\Lambda}) \leq \mathbb{G}(R) \tag{23}$$

for *any* choice of $\mathcal{C} = \{\mathscr{C}_1, \mathscr{C}_2, \ldots, \mathscr{C}_\theta\}$ and $\mathbf{\Lambda}$ corresponding to a rate R.

[10] In this context, a column is called "independent" when it is linearly independent of all the other matrix columns.

Proof: For given $\mathcal{C} = \{\mathscr{C}_1, \mathscr{C}_2, \ldots, \mathscr{C}_\theta\}$ and $\mathbf{\Lambda}$, the evolution of the probabilities (p_ℓ, q_ℓ) is governed by the recursions $q_\ell = f_{\mathsf{b}}(p_{\ell-1})$ and $p_\ell = f_{\mathsf{s}}(q_\ell)$ in (5) and (8), for all $\ell \geq 1$ and with $q_1 = f_{\mathsf{b}}(0)$. Let us denote the areas below the BN and the SN EXIT functions over the interval $[0,1]$ by

$$A_{\mathsf{b}} = \int_0^1 f_{\mathsf{b}}(p) \mathrm{d}p$$

and

$$A_{\mathsf{s}} = \int_0^1 f_{\mathsf{s}}(q) \mathrm{d}q$$

respectively. (These two areas are highlighted in the example EXIT chart depicted in Fig. 4.) A necessary and sufficient condition for successful decoding is represented by the existence of an "open tunnel" between the two curves in the EXIT chart, which necessarily implies[11]

$$A_{\mathsf{b}} + A_{\mathsf{s}} \leq 1 \,. \tag{24}$$

In particular, (24) must be satisfied for $G = G^*(\mathcal{C}, \mathbf{\Lambda})$. The area below the SN EXIT function (8) is given by

$$A_{\mathsf{s}} = 1 + \frac{R}{G} e^{-\frac{G}{R}} - \frac{R}{G} \,. \tag{25}$$

Moreover, the area below the BN EXIT function (5) is given by

$$\begin{aligned} A_{\mathsf{b}} &= \sum_{h=1}^{\theta} \lambda_h \int_0^1 f_{\mathsf{b}}^{(h)}(p) \mathrm{d}p \\ &\overset{\text{(a)}}{=} \sum_{h=1}^{\theta} \lambda_h \frac{k}{n_h} \\ &\overset{\text{(b)}}{=} R \end{aligned} \tag{26}$$

where (a) follows from the Area Theorem [33] and holds under the assumption of MAP erasure decoding at the burst node[12], and where (b) is due to $\lambda_h = \frac{n_h \Lambda_h}{\bar{n}}$, to $\sum_{h=1}^{\theta} \Lambda_h = 1$, and to (3). By incorporating (25) and (26) in (24) we obtain

$$R + \frac{R}{G} e^{-G/R} \leq \frac{R}{G}$$

which may be recast as

$$R(G) \geq -\frac{G}{\log(1-G)} \,. \tag{27}$$

Next, define $\mathbb{G}(R)$ as the unique solution in $(0,1]$ of (22), yielding $R(\mathbb{G}) = -\mathbb{G}/\log(1-\mathbb{G})$. Since (27) must hold in particular for $G = G^*(\mathcal{C}, \mathbf{\Lambda})$ and since the function $y = -x/\log(1-x)$, $x \in [0,1)$, is monotonically decreasing, we obtain (23). ■

Note that, while $G^*(\mathcal{C}, \mathbf{\Lambda})$ depends on R through $\mathcal{C}$ and $\mathbf{\Lambda}$, its upper bound $\mathbb{G}(R)$ depends solely on R. An alternative proof of the upper bound (23) is proposed in Appendix B. It is manifest from the alternative proof that, for any rate R, the

[11] Inequality (24) is a necessary but not sufficient condition for successful decoding.

[12] The Area Theorem states that the area below the MAP EXIT function of a linear block code without idle symbols equals its code rate.

asymptotic throughput cannot exceed the value $\mathbb{G}(R)$ even if a "genie-aided" decoding approach, consisting of solving the linear system of equations via Gaussian elimination, is followed.

V. Design and Analysis of CSA Random Access Schemes

In this section, numerical results on CSA access schemes are illustrated. The section is divided into two parts. The objective of the first part (Section V-A) is to show that the asymptotic tools developed in Section III may confidently be used to design access schemes for a finite MAC frame size. In the process, CSA schemes based on simple codes of dimensions $k = 2$ and $k = 3$ are compared with IRSA schemes. Purpose of Section V-A is also to highlight the rate region in which CSA schemes provide advantages over IRSA ones and the rate region in which IRSA protocols are preferable. The second part of the section (Section V-B) is devoted to the design of CSA probability distributions approaching the bound established by Theorem 4.1.

A. Performance Analysis of Finite-Length CSA Schemes

The analysis tool developed in Section III-A allows to calculate the threshold $G^*(\mathcal{C}, \mathbf{\Lambda})$ for a given choice of the θ linear block component codes $\mathscr{C}_h$, $h \in \{1, \ldots, \theta\}$, and of the p.m.f. $\mathbf{\Lambda}$. Analogously, the tool developed in Section III-C allows to evaluate the threshold $G^*(\mathscr{N}, \mathbf{\Lambda})$ of a CSA scheme under the random code hypothesis, for a given choice of the codeword lengths n_s, $s \in \{1, \ldots, s_{\max}\}$, and of the p.m.f. $\mathbf{\Lambda}$. These tools can be exploited to derive optimal (in the sense of maximizing the threshold) probability distributions $\mathbf{\Lambda}$ in the two cases.

Some optimized probability distributions, obtained applying the random code hypothesis, are shown in Table I. Among the several possible algorithms available to find the global maximum of a nonlinear function, differential evolution [37] has been used (with the exception of the $R = 1/2$ IRSA scheme, for which the only possibility is that all users employ a $(2, 1)$ repetition code). In the upper part of the table, p.m.f.s $\mathbf{\Lambda}$ are reported for IRSA schemes with rates $1/2$, $2/5$, and $1/3$, while in the lower part p.m.f.s $\mathbf{\Lambda}$ are detailed for CSA schemes with $k = 2$ and $k = 3$ and with the same rates, with the inclusion of $R = 3/5$. All distributions have been optimized under the constraint that the smallest local rate allowed for each user is $1/6$. For each IRSA distribution the threshold $G^*(\mathcal{C}, \mathbf{\Lambda})$ and the corresponding stability bound are shown. On the other hand, for each CSA distribution both the threshold $G^*(\mathscr{N}, \mathbf{\Lambda})$ under the random code hypothesis and the corresponding stability bound, are reported. For all rates R, the value of the capacity bound $\mathbb{G}(R)$ is shown in the last row of the table.

Table II shows the thresholds $G^*(\mathcal{C}, \mathbf{\Lambda})$ for CSA schemes with $k = 2$ and characterized by the same p.m.f.s $\mathbf{\Lambda}$ as the ones in Table I, but for a specific choice of the component codes. More in detail, these thresholds have been obtained using linear block component codes generated by the following generator matrices:

$$\mathbf{G}_{(3,2)} = [110, 011]$$
$$\mathbf{G}^{(a)}_{(4,2)} = [1100, 1111]$$
$$\mathbf{G}^{(b)}_{(4,2)} = [1100, 0111]$$
$$\mathbf{G}^{(a)}_{(5,2)} = [11100, 00111]$$
$$\mathbf{G}^{(b)}_{(5,2)} = [11110, 00011]$$

TABLE I
IRSA p.m.f.s $\mathbf{\Lambda}$ with rates $1/3$, $2/5$, and $1/2$, and CSA p.m.f.s $\mathbf{\Lambda}$ for $k = 2, 3$ with rates $1/3$, $2/5$, $1/2$, and $3/5$, under the random code hypothesis.

IRSA				
	$R = 1/3$	$R = 2/5$	$R = 1/2$	
$(2, 1)$	0.554016	0.622412	1.000000	
$(3, 1)$	0.261312	0.255176		
$(4, 1)$		0.122412		
$(6, 1)$	0.184672			
$G^*(\mathcal{C}, \mathbf{\Lambda})$	0.8792	0.7825	0.5000	
$G^*_{\mathsf{sb}}(\mathcal{C}, \mathbf{\Lambda})$	0.9025	0.8033	0.5000	
CSA $k = 2$, random component codes				
	$R = 1/3$	$R = 2/5$	$R = 1/2$	$R = 3/5$
$(3, 2)$	0.259929	0.304961		0.666667
$(4, 2)$	0.053247	0.144152	1.000000	0.333333
$(5, 2)$	0.447058			
$(6, 2)$		0.347701		
$(7, 2)$		0.203186		
$(11, 2)$	0.105258			
$(12, 2)$	0.134509			
$G^*(\mathscr{N}, \mathbf{\Lambda})$	0.9034	0.8185	0.6556	0.4091
$G^*_{\mathsf{sb}}(\mathscr{N}, \mathbf{\Lambda})$	0.9035	0.8185	0.7500	0.4091
CSA $k = 3$, random component codes				
	$R = 1/3$	$R = 2/5$	$R = 1/2$	$R = 3/5$
$(4, 3)$	0.173572		0.045538	
$(5, 3)$	0.010699	0.579066		1.000000
$(6, 3)$	0.183304		0.863386	
$(7, 3)$	0.361921		0.091076	
$(8, 3)$	0.025012			
$(10, 3)$		0.025606		
$(11, 3)$		0.395328		
$(18, 3)$	0.245492			
$G^*(\mathscr{N}, \mathbf{\Lambda})$	0.9107	0.8386	0.6868	0.5078
$G^*_{\mathsf{sb}}(\mathscr{N}, \mathbf{\Lambda})$	0.9143	0.8918	0.9227	0.5250
$\mathbb{G}(R)$	0.9405	0.8926	0.7968	0.6758

TABLE II
CSA p.m.f.s $\mathbf{\Lambda}$ for $k = 2$ with rates $1/3$, $2/5$, $1/2$, and $3/5$, for a specific choice of the component codes.

CSA $k = 2$, specific component codes				
	$R = 1/3$	$R = 2/5$	$R = 1/2$	$R = 3/5$
$(3, 2)$	0.259929	0.304961		0.666667
$(4, 2)_{(a)}$	0.053247	0.144152		
$(4, 2)_{(b)}$			1.000000	0.333333
$(5, 2)_{(a)}$	0.259293			
$(5, 2)_{(b)}$	0.098353			
$(5, 2)_{(c)}$	0.089412			
$(6, 2)$		0.347701		
$(7, 2)$		0.203186		
$(11, 2)$	0.105258			
$(12, 2)$	0.134509			
$G^*(\mathcal{C}, \mathbf{\Lambda})$	0.9030	0.8229	0.6793	0.4286
$G^*_{\mathsf{sb}}(\mathcal{C}, \mathbf{\Lambda})$	0.9241	0.8311	1.0000	0.4286

$$\begin{aligned}
\mathbf{G}^{(c)}_{(5,2)} &= [11111, 00011] \\
\mathbf{G}_{(6,2)} &= [111000, 001111] \\
\mathbf{G}_{(7,2)} &= [1111000, 0011111] \\
\mathbf{G}_{(11,2)} &= [11110000000, 00111111111] \\
\mathbf{G}_{(12,2)} &= [111111110000, 000001111111] \,. \qquad (28)
\end{aligned}$$

Note that this specific choice of the codes $\mathscr{C}_h$ leads to thresholds $G^*(\mathcal{C}, \mathbf{\Lambda})$ which are either slightly larger than the corresponding ones in Table I or practically coincident with them (as it is the case for the the rate-$1/3$ scheme). Also note that in CSA, it is possible to combine different component codes having the same dimension and length. This is the case, for instance, of the $R = 1/3$ scheme in Table II in which three different $(5, 2)$ component codes are combined. The sum of the probabilities with which these three codes are picked by each user is equal to 0.447058, the value in Table I designed using the random code approach. For completeness, the EXIT charts relevant to the $R = 1/3$ IRSA configuration in Table I and to the $R = 1/3$ CSA scheme in Table II are depicted in Fig. 5(a) and Fig. 5(b), respectively.

As it was previously highlighted, CSA allows to construct uncoordinated access schemes with any rate $0 < R < 1$, whereas only rates $0 < R \leq 1/2$ can be obtained with IRSA, unless some users transmit their burst in the MAC frame with no repetition.[13] (This is the reason for the optimized CSA distributions of rate $R = 3/5$ in Table I have no IRSA counterpart.) Furthermore, from Table I and Table II we see that CSA is capable to achieve better performance than IRSA, in terms of asymptotic thresholds, over the whole range of rates $1/3 \leq R \leq 1/2$, and that the threshold values achieved by CSA schemes are *substantially* better than the ones achieved by IRSA for values of R that are close to $1/2$. For example, for $R = 1/3$ a threshold $G^*(\mathscr{N}, \mathbf{\Lambda}) = 0.9143$ is achieved by the best found CSA scheme with $k = 3$ (under the random code approach), whereas the best found IRSA threshold is $G^*(\mathcal{C}, \mathbf{\Lambda}) = 0.8792$. For rate $R = 1/2$ the improvement is much more pronounced, the threshold achieved by the best found CSA scheme with $k = 3$ (under the random code approach) being $G^*(\mathscr{N}, \mathbf{\Lambda}) = 0.6868$ and the one achieved by IRSA being $G^*(\mathcal{C}, \mathbf{\Lambda}) = 0.5000$.

For all tested values of R we have observed improvements in terms of asymptotic threshold when the dimension k of the component codes increases. This improvement becomes however almost negligible for low rates R (equivalently, for high values of the excess energy $\Delta E = -10 \log_{10} R$), a regime in which it is possible to design IRSA schemes based on simple repetition codes, with thresholds very close to the upper bound $\mathbb{G}(R)$ (an example is represented by the distribution $\Lambda_1(x)$ that will be presented in Section V-B). Simplifying, we may conclude that for rates $R < 1/3$ the IRSA protocols should be preferred to CSA ones, as their design is simpler and the gain provided by CSA is limited. On the other hand, CSA protocols are more appealing and effective than IRSA ones in the range $1/3 \leq R \leq 1/2$ (where a higher energy efficiency is required) due to their better thresholds exhibited by the corresponding optimized distributions. CSA schemes are a mandatory choice for $R > 1/2$. For CSA protocols, higher values of k are effective in improving the threshold, as discussed further in Section V-B.

[13] In case the set $\mathcal{C}$ for an IRSA scheme includes repetition codes of length 1, however, successful IIS can never be guaranteed due to the impossibility to subtract the interference of two bursts colliding in a slot and that have no replicas in other slots. As a consequence, density evolution recursion (13) will not converge to zero for any value of π always yielding $G(\mathcal{C}, \mathbf{\Lambda})^* = 0$.

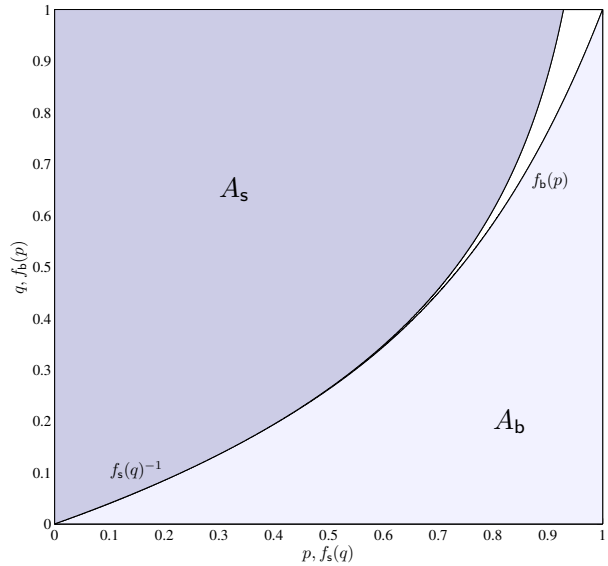

(a)

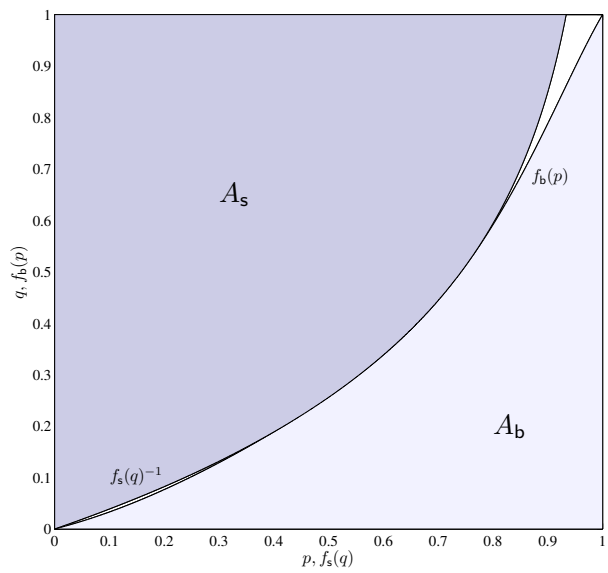

(b)

Fig. 5. EXIT charts for the $R = 1/3$ IRSA scheme in Table I and for the $R = 1/3$ CSA scheme with $k = 2$ in Table II. The EXIT chart of the CSA scheme is obtained with the choice (28) of the component code generator matrices.

To validate our design approach based on the asymptotic analysis, we performed numerical simulations for finite frame size M and user population size N. In Fig. 6(a) and Fig. 6(b), the throughput curves without retransmissions of IRSA schemes in Table I and of CSA ($k = 2$) schemes in Table II are depicted as functions of the expected channel

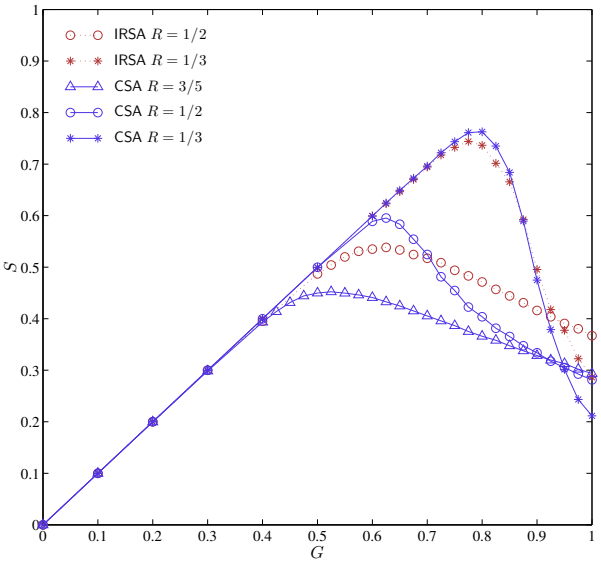

(a)

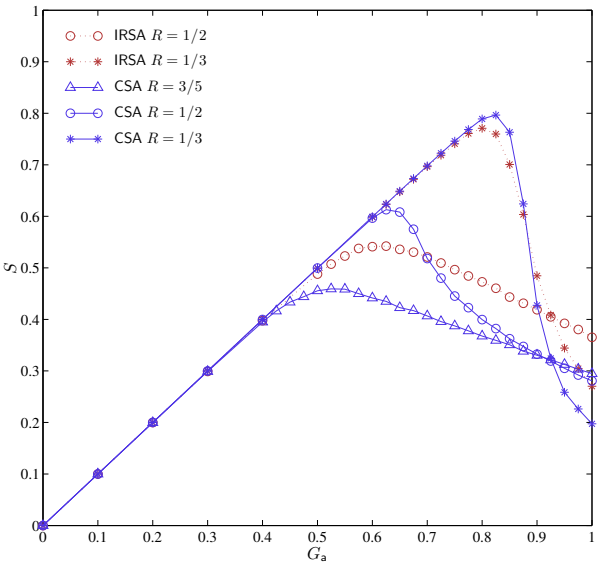

(b)

Fig. 6. Throughput S versus (a) the expected and (b) the instantaneous channel load for IRSA and CSA ($k = 2$) configurations with p.m.f.s $\mathbf{\Lambda}$ in Table I and Table II, respectively. The linear block codes whose generator matrices are detailed in (28) are employed for the CSA case.

load G and of the instantaneous channel load G_{a}, respectively, for $R \in \{1/3, 1/2, 3/5\}$. In our simulations for the CSA schemes, we used the linear block component codes generated by the generator matrices detailed in (28). For the sake of fairness, we compared CSA ($k = 2$) and IRSA schemes for the same frame duration T_{frame} which implies $T_{\mathsf{slot}} = 2\,T_{\mathsf{segment}}$, i.e., a number of slices twice the number of slots. Specifically, the simulations are for $T_{\mathsf{frame}}/T_{\mathsf{segment}} = 1000$

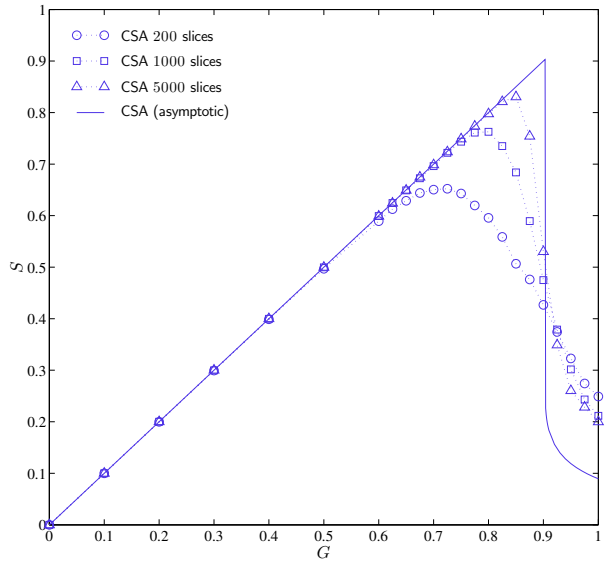

Fig. 7. Asymptotic throughput curve for the $R = 1/3$ CSA configuration in Table II and throughput curves for the same configuration under different lengths (in slices) of the MAC frame. Population size $N = 20000$.

slices and $T_{\mathsf{frame}}/T_{\mathsf{slot}} = 500$ slots.[14] All simulations have been conducted for a population $N = 20000$ users. The activation probability π corresponding to each value of the expected channel load G in Fig. 6(a) may be obtained as $\pi = G\,M/N$, while the number of active users for each value of the instantaneous load G_{a} in Fig. 6(b) as $N_{\mathsf{a}} = G_{\mathsf{a}} M$. We can observe how the trend of the peak throughput values measured in the finite length case follow the same trend predicted by the asymptotic analysis. In particular, the slightly larger peak throughput exhibited by CSA (for the specific choice of the component codes) for $R = 1/3$ is in agreement with the thresholds reported in Table I and Table II.

For a given set $\mathcal{C}$ of component codes and a given p.m.f. $\mathbf{\Lambda}$, the threshold $G^*(\mathcal{C}, \mathbf{\Lambda})$ represents the asymptotic peak throughput of the corresponding CSA scheme (in the limit where M tends to infinity). In Fig. 7 the asymptotic throughput curve (versus the expected channel load G) of the rate $R = 1/3$ CSA scheme from Table II, with the component codes detailed in (28), is compared with the throughput curves obtained by numerical simulation for the same $(\mathcal{C}, \mathbf{\Lambda})$ pair, for $M = 100$, 500, and 2500 slots (corresponding, for $k = 2$, to 200, 1000, and 5000 slices, respectively), always assuming $N = 20000$ users. From this figure it is possible to appreciate how the curves for a finite number of slots tend to better and better fit the asymptotic curve as the number of slots increases.

B. Approaching the Capacity Bound

In this subsection we consider the problem of designing CSA configurations whose asymptotic thresholds approach

[14] It should be considered that each segment has to be encoded via a physical layer error correcting code before transmission on the MAC channel, and that the physical layer code for CSA is k times shorter than the corresponding code for IRSA. Thus, CSA may require working at slightly higher SNRs than IRSA, especially when short segments (and then short physical layer codes) are used. This aspect is not captured by our collision channel model.

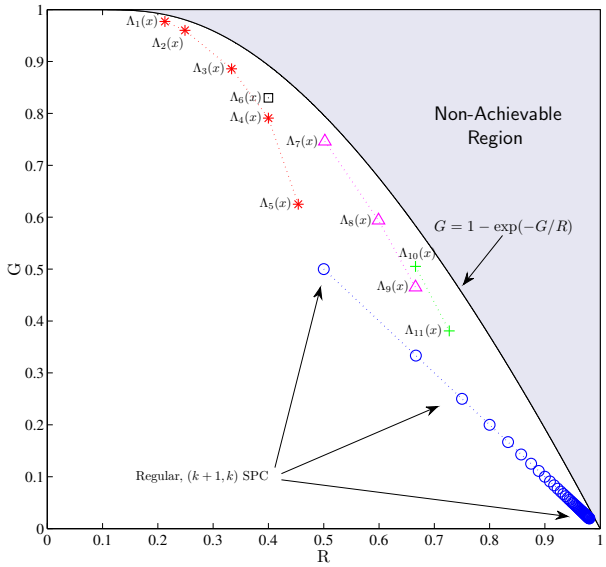

Fig. 8. Upper bound to the capacity vs. rate R. Thresholds G^* are reported for selected distributions. Distributions $\Lambda_i(x), i = 1, \ldots, 5$ ($*$) are IRSA configurations based on repetition codes ($k = 1$). Distribution $\Lambda_6(x)$ ($\square$) is based on MDS codes with $k = 2$. Distributions $\Lambda_i(x), i = 7, 8, 9$ ($\triangle$) are based on MDS codes with $k = 3$. Distributions $\Lambda_i(x), i = 10, 11$ ($+$) are based on MDS codes with $k = 4$. Distributions based on $(k + 1, k)$ SPC codes are also displayed ($\circ$).

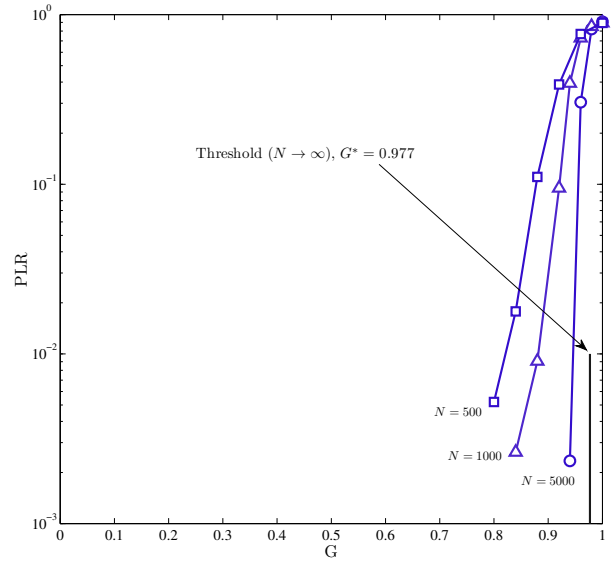

Fig. 9. Packet loss rate for the CSA scheme based on the distribution $\Lambda_1(x)$. $N = 5000, 1000, 500$, maximum iteration count set to 100.

the upper bound in Theorem 4.1. To do so, for a given k, a given set $\mathcal{C} = \{\mathscr{C}_1, \mathscr{C}_2, \ldots, \mathscr{C}_\theta\}$ of component codes, and a given target rate R, we search (again via differential evolution optimization) the distribution $\mathbf{\Lambda}$ which maximizes $G^*(\mathcal{C}, \mathbf{\Lambda})$. In order to limit the search space, we focus on schemes based on codes of moderate-low length. We resort on a compact polynomial notation to specify the developed p.m.f.s $\mathbf{\Lambda} = \{\Lambda_h\}_{h=1}^{\theta}$. This notation is introduced for each specific case before its usage.

Based on the observations in Section V-A, we start by designing some low-rate IRSA schemes, in which case we define $\Lambda(x) = \sum_h \Lambda_h x^h$, where $\mathscr{C}_h$ is the $(h, 1)$ repetition code. Selecting a rate $R = 1/5$ and limiting the maximum length of the repetition component codes to 30 (i.e., considering only repetition codes with rate down to $1/30$), we obtain the distribution

$$\begin{aligned}\Lambda_1(x) = {} & 0.494155x^2 + 0.159085x^3 + 0.107372x^4 \\ & + 0.070336x^5 + 0.045493x^6 + 0.019898x^7 \\ & + 0.024098x^{11} + 0.008636x^{12} + 0.005940x^{13} \\ & + 0.008749x^{15} + 0.002225x^{18} + 0.001261x^{20} \\ & + 0.002607x^{22} + 0.008092x^{23} + 0.002287x^{24} \\ & + 0.012274x^{25} + 0.002530x^{26} + 0.003094x^{27} \\ & + 0.002558x^{28} + 0.005891x^{29} + 0.013419x^{30}\end{aligned}$$

whose threshold is $G^*(\mathcal{C}_1, \mathbf{\Lambda}_1) = 0.977$. The corresponding point on the G versus R plane is reported in Fig. 8 and compared with the bound given by Theorem 4.1. On the same chart the points corresponding to IRSA distributions with different rates, denoted by $\Lambda_i(x)$ for $i \in \{2, \ldots, 5\}$, are reported. Whereas for low rates R repetition-based configurations approach the bound quite tightly, for rates close to $1/2$ they show visible losses. For example, the distribution

$$\Lambda_5(x) = 0.8x^2 + 0.2x^3$$

(obtained constraining the maximum length of the component codes to $n_h = 5$) is characterized by a rate $R = 5/11$ and attains a threshold $G^*(\mathcal{C}_5, \mathbf{\Lambda}_5) = 0.625$, whereas $\mathbb{G}(5/11) = 0.843$. This effect if somehow expected since in the limiting case of $R = 1/2$, in which each user employs a $(2, 1)$ repetition code, the corresponding threshold is limited to 0.5.

Fig. 9 shows the packet loss rate (PLR) achieved by the scheme employing the distribution $\Lambda_1(x)$ without retransmissions. The results have been derived via Monte Carlo simulations for MAC frames of size $M = 5000$, 1000, and 500 slots, and are compared with the capacity of the scheme, $G^*(\mathcal{C}_1, \mathbf{\Lambda}_1) = 0.977$. For the $M = 5000$ case, a PLR close to 2×10^{-3} is achieved at a channel traffic $G = 0.94$ [packets/slot], only 0.05 [packets/slot] away from the bound established by Theorem 4.1 ($\simeq 0.99$ [packets/slot]).

As observed in Section V-A, when the rate R is not too low, e.g., $R \geq 1/3$, it becomes convenient to adopt component codes with $k > 1$. To this purpose, we designed CSA schemes where each $\mathscr{C}_h \in \mathcal{C}$ is an MDS code constructed on an appropriate non-binary finite field,[15] for component code dimensions $k = 2$, 3, and 4. It is assumed that each burst node locally adopts a bounded-distance decoding strategy at each iteration, consisting of recovering the lost encoded segments connected to it only if the current number of its collision-free received segments is at least k. Under this assumption, the EXIT function of a BN using an (n_h, k) MDS codes is

[15] Imposing limits on n_h, this approach is realistic. For instance, (generalized) Reed-Solomon codes on finite fields of moderate order may be used.

TABLE III
CSA DISTRIBUTIONS FOR $k \in \{2,3,4\}$ AND CORRESPONDING ASYMPTOTIC THRESHOLDS. ALL CONFIGURATIONS ARE BASED ON MDS CODES.

	R	$\Lambda(x)$	$G^*(\mathcal{C},\mathbf{\Lambda})$	$\mathbb{G}(R)$
$k=2$	0.400	$\Lambda_6(x) = 0.276023x + 0.366641x^2 + 0.127979x^3 + 0.229357x^7$	0.830	0.893
$k=3$	0.502	$\Lambda_7(x) = 0.3222x + 0.2305x^2 + 0.0491x^4 + 0.3983x^5$	0.746	0.795
	0.599	$\Lambda_8(x) = 0.2589x + 0.4826x^2 + 0.2586x^3$	0.594	0.677
	0.667	$\Lambda_9(x) = 0.5005x + 0.4995x^2$	0.465	0.582
$k=4$	0.667	$\Lambda_{10}(x) = 0.1892x + 0.6240x^2 + 0.1868x^3$	0.505	0.582
	0.727	$\Lambda_{11}(x) = 0.5000x + 0.5000x^2$	0.381	0.491

given by

$$f_{\mathsf{b}}^{(h)}(p) = \sum_{l=0}^{k-1} \binom{n_h - 1}{l} (1-p)^l p^{n_h - l - 1}. \tag{29}$$

In this case, we specify the CSA p.m.f.s $\mathbf{\Lambda}$ via the compact polynomial notation $\Lambda(x) = \sum_h \Lambda_h x^h$, where $\mathscr{C}_h$ is an $(h+k, k)$ MDS code. The obtained CSA distributions are reported in Table III.

For $k = 2$ and $R = 0.4$ we designed the distribution $\Lambda_6(x)$ characterized by a threshold $G^*(\mathcal{C}_6, \mathbf{\Lambda}_6) = 0.830$. For the same rate, the best found IRSA configuration for a maximum n_h set to 10 ($\Lambda_4(x)$ in Fig. 8), achieves $G^*(\mathcal{C}_4, \mathbf{\Lambda}_4) = 0.791$ while the best found CSA ($k = 2$) scheme based on binary codes in Table II achieves $G^*(\mathcal{C}, \mathbf{\Lambda}) = 0.8229$. Moving to the moderate-rate regime, we observed that, also employing MDS codes under bounded distance decoding as component codes, for the same rate R the bound $\mathbb{G}(R)$ can be better approached resorting on CSA distributions based on higher code dimensions k (see Fig. 8), at the expense of a higher local decoding complexity. For example, for $R = 0.667$ the distribution $\Lambda_9(x)$ (based on $k = 3$) achieves $G^*(\mathcal{C}_9, \mathbf{\Lambda}_9) = 0.465$, whereas $G^*(\mathcal{C}_{10}, \mathbf{\Lambda}_{10}) = 0.505$ is achieved by the distribution $\Lambda_{10}(x)$ (based on $k = 4$). In Fig. 8 the thresholds achieved by regular schemes based on SPC codes of increasing rates are also shown. As k grows the rate of these scheme approaches 1 and the corresponding threshold $1/(k+1)$ tends to 0. For large k, the scheme tends to operate close to the capacity bound for very high rates.

VI. CONCLUSIONS

In this paper, a coding approach relying on iterative interference subtraction for the collision channel without feedback has been proposed and analyzed. The scheme, dubbed CSA, can be seen as an extension of the IRSA scheme, where the extension consists of splitting packets into segments and encoding the segments via randomly picked local component codes. A bridge between erasure decoding for graph-based codes and the iterative interference cancellation process of CSA has been established, allowing an elegant analysis of the access scheme performance. Exploiting this graphical representation, density evolution equations for CSA on the collision channel have been obtained and used to analyze the iterative interference subtraction process. The "capacity" of the CSA scheme without retransmissions has been defined and, in the process, it has been shown that the scheme is asymptotically reliable even if retransmissions are forbidden. A throughput as high as $1\,[\text{packets/slot}]$ has been shown to be tightly approachable when sufficiently low coding rates are employed for the component codes. Furthermore, a technique to design CSA schemes with arbitrarily high coding rates has been developed which allows approaching the capacity bound over the whole range of rates. Numerical results have been presented to validate the proposed analytical framework.

We conclude this paper by discussing some possible directions of further investigation emerging from the presented results. Considering the same collision channel model adopted in the present paper, for example, the analogy with iterative decoding on the erasure channel suggests that it might be possible to develop sequences of CSA configurations achieving the capacity bound (23) for any value of the rate R, similarly to the well-known LDPC "capacity-achieving sequences" [36]. We conjecture that, provided such sequences exist, their construction requires an increasing value of the component codes dimension k. Considering again the collision channel, the extra-ordinary performances obtained in the LDPC coding context by exploiting spatial coupling [38] prompt the adoption of this paradigm toward the design of "convolutional" CSA schemes. (The only paper we are aware of in this context is [39] in which, however, only spatially coupled IRSA configurations have been addressed.) Interesting directions of investigation also arise both from introducing spatial diversity through the assumption of availability of multiple receivers (as was done in [40] for pure slotted ALOHA) and from abandoning the simple collision channel model to consider the more general MPR model. Some work in this sense has already been carried out in [41], in the framework of CRDSA exploiting the capture effect, and in [42], in the framework of IRSA with multiuser detection.

APPENDIX A
RESULTS ON SUCCESSIVE INTERFERENCE CANCELLATION

In this appendix we address the actual performance achievable under a realistic SIC scheme. More specifically, we intend to validate the assumption that, after removing $l-1$ interfering segments from a slice in which l segments collided, the remaining segment can be decoded correctly with very high probability. In practice, this turns into verifying that the residual interference after interference cancellation (due to imperfect channel estimation) does not degrade considerably the performance of the error correcting code used to protect the segments.

To this purpose, let's consider the case where l users attempt a segment transmission within the same slice. We

stick to the case of perfect power control and equal channel condition (gain) among the users. We denote by $u^{(i)}(t)$ the complex baseband pulse amplitude modulation (PAM) signal transmitted by the i-th user, i.e.,

$$u^{(i)}(t) = \sum_{v=1}^{N_s} b_v^{(i)} \gamma(t - vT_s)$$

where N_s is the number of symbols per segment, $\{b_v^{(i)}\}$ is the sequence of such symbols and T_s is the symbol period. By $\gamma(t) = \mathcal{F}^{-1}\left\{\sqrt{\mathtt{RC}(f)}\right\}$ we denote the pulse shape, where $\mathtt{RC}(f)$ the frequency response of the raised-cosine filter.

Each contribution is received with a random delay ϵ_i, a random frequency offset $f_i \sim \mathcal{U}[-f_{\max}, f_{\max}]$ and a random phase offset $\phi_i \sim \mathcal{U}[0, 2\pi)$. The received signal after the matched filter (MF) is given by $r(t) = \sum_{i=1}^{l} z^{(i)}(t) * h(t) + n(t)$ where $n(t)$ is the Gaussian noise contribution, $h(t) = \gamma^*(-t)$ is the MF impulse response and $z^{(i)}(t) = \sum_{v=1}^{N_s} b_v^{(i)} \gamma(t - vT_s - \epsilon_i) \exp(j2\pi f_i t + j\phi_i)$. Assuming frequency shifts that are small w.r.t. the signal bandwidth (i.e., $f_{\max} T_s \ll 1$), the received signal may be approximated by

$$r(t) \approx \sum_{i=1}^{l} \tilde{u}^{(i)}(t - \epsilon_i) e^{j2\pi f_i t + j\phi_i} + n(t) \tag{30}$$

where $\tilde{u}^{(i)}(t)$ is the response of the MF to $u^{(i)}(t)$. In the following we regard $\tilde{u}^{(1)}(t)$ as the useful term and $\tilde{u}^{(2)}(t), \tilde{u}^{(3)}(t), \ldots, \tilde{u}^{(l)}(t)$ as the interference to be cancelled. These latter $l-1$ terms are assumed to have been successfully recovered via MAP erasure decoding of the associated component code.

To proceed with SIC, it is necessary to estimate the set of parameters $\{\epsilon_i, f_i, \phi_i\}$, for $i \in \{2, \ldots, l\}$. As suggested in [11], we consider the case where ϵ_i and f_i can be accurately estimated on the segments of the same burst that have already been recovered, and that their values remain constant through the frame. As pointed out in [11], this argument does not hold for the phase rotation terms ϕ_i, which may not be stable from a slice to another one. As such, we need to estimate ϕ_i for each segment individually and directly on the slice where we want to eliminate its contribution. A fine phase estimation can be obtained by a data aided approach. Recall in fact that the symbol sequences $\{b_v^{(i)}\}$ (for $i \in \{2 \ldots l\}$) are known at the receiver, since they can be reconstructed after MAP erasure decoding of the associated component code. The SIC works as follows. We denote by $y^{(i)}(t)$ the signal at the input of the phase estimator for the i-th contribution. In the first step, the input signal is given by $y^{(2)}(t) = r(t)$ and the phase of the first interfering user ($i = 2$) is estimated as

$$\hat{\phi}_2 = \arg\left\{\sum_{v=1}^{N_s} y_v^{(2)} \left(b_v^{(2)}\right)^*\right\}$$

with

$$y_v^{(2)} = y^{(2)}(vT_s + \epsilon_2) e^{-j2\pi f_2 (vT_s + \epsilon_2)}.$$

After the estimation of the phase offset for the first interferer, the corresponding signal can be reconstructed as $\tilde{u}^{(2)}(t - \epsilon_2) e^{j2\pi f_2 t + j\hat{\phi}_2}$ and its contribution can be removed from (30), i.e.

$$y^{(3)}(t) = y^{(2)}(t) - \tilde{u}^{(2)}(t - \epsilon_2) e^{j2\pi f_2 t + j\hat{\phi}_2}.$$

The SIC proceeds serially. For the generic i-th contribution we have

$$\hat{\phi}_i = \arg\left\{\sum_{v=1}^{N_s} y_v^{(i)} \left(b_v^{(i)}\right)^*\right\} \tag{31}$$

with $y_v^{(i)} = y^{(i)}(vT_s + \epsilon_i) \exp\left(-j2\pi f_i (vT_s + \epsilon_i)\right)$ and

$$y^{(i)}(t) = y^{(i-1)}(t) - \tilde{u}^{(i-1)}(t - \epsilon_{i-1}) e^{j2\pi f_{i-1} t + j\hat{\phi}_{i-1}}.$$

After the cancellation of the $l-1$ contributions the residual signal, denoted by $y^{(1)}(t)$, is given by the 1-st user's contribution, the noise $n(t)$, and a residual interference term $\nu(t)$ due to the imperfect estimation of the interferers' phases (causing imperfect SIC), i.e.,

$$y^{(1)}(t) = \tilde{u}^{(1)}(t - \epsilon_1) e^{j2\pi f_1 t + j\phi_1} + n(t) + \nu(t). \tag{32}$$

The estimation of $\{\epsilon_1, f_1, \phi_1\}$ is then performed on the signal in (32). After sampling, soft-demodulation takes place, and the log-likelihood ratios for the codeword bits are derived. This data aided approach works if the cross-correlation between the sequences $\{b_v^{(i)}\}$, $i \in \{1 \ldots l\}$, is on average low, which is the case if each user encodes segments whose bits can be modeled as independent and identically distributed (i.i.d.) random variables.

We simulated the SIC process with various numbers of collisions. The information sequences were randomly generated, then encoded through a $(512, 256)$ cycle code from [43] over $\mathbb{F}_{256}$. Quadrature phase-shift keying (QPSK) modulation was considered for the simulations. For each transmission attempt we generated the parameters $\{\epsilon_i, f_i, \phi_i\}$ according to the distributions presented before, with maximum frequency shift $f_{\max} = 0.01/T_s$. The received signal $r(t)$ has then been oversampled at a rate M_s/T_s with $M_s = 8$, and the SIC algorithm has been applied to the oversampled digital signal.

Once the $l-1$ interference contributions have been cancelled, log-likelihood ratios for the codeword bits have been input to the channel decoder. In Fig. 10 the impact of the SIC process on the block error rate for the segment to be recovered (i.e., the signal corresponding to $i = 1$) is shown in terms of block error rate vs. E_b/N_0 for $l = 2, 4, 6, 8$ segment collisions (i.e., $1, 3, 5, 7$ interferers). The performance on the additive white Gaussian noise (AWGN) channel without collisions is provided as reference. Note that, up to $l = 8$ collisions, the performance degradation due to the imperfect estimation of the phase offsets is small, namely, less than 1 dB at block error rate $\simeq 10^{-3}$. Considering $E_b/N_0 = 2.5$ dB, after removing $l-1 = 7$ interference contributions we have a block error rate close to 10^{-2}.

Appendix B
An alternative Proof of the Capacity Bound (23)

In this appendix, we propose an alternative proof of the upper bound (23). This proof is based on adopting an equivalent channel model that is addressed next.

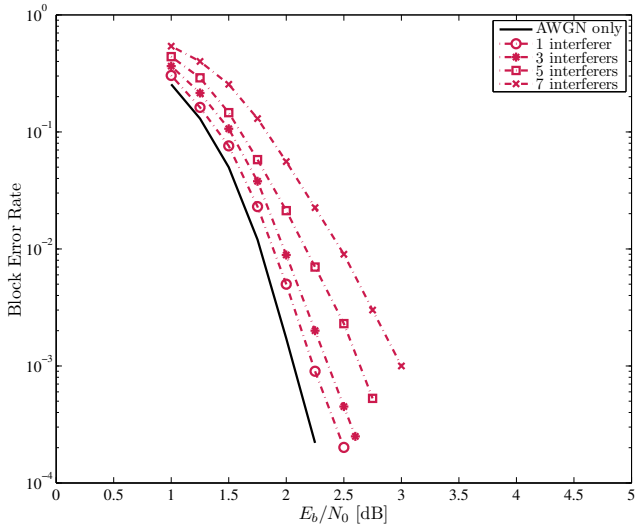

Fig. 10. Block error rate vs. E_b/N_0 for a $(512, 256)$ cycle code with QPSK modulation, 50 iterations of the belief propagation algorithm. Various number of interferers.

Encoded segments are packets of bits that can be mapped onto the elements of a finite field $\mathrm{GF}(2^l)$, for appropriate integer l. We model collisions between segments as sums of symbols in $\mathrm{GF}(2^l)$. In each slice of the MAC frame the decoder is capable to discriminate between a "silence" (no active user has transmitted in that segment), a symbol in $\mathrm{GF}(2^l)$ corresponding to a unique slice, or a symbol in $\mathrm{GF}(2^l)$ being the result of a collision. In this latter case, the observed symbol in $\mathrm{GF}(2^l)$ provides no information to the decoder about the number and the values of colliding segments.

As such, with respect to the channel model discussed in Section II-C, Assumption 1 and Assumption 2 remain valid, while Assumption 3 is replaced by the following equivalent assumption (in that all developed results still hold):

Assumption 4: If a collision occurs between $d > 1$ slices $s_1, s_2, \ldots, s_d \in \mathrm{GF}(2^l)$, the symbol $s = s_1 + s_2 + \cdots + s_d \in \mathrm{GF}(2^l)$ is generated in the corresponding segment of the frame. Cancellation of the interference contribution of a segment consists of adding the corresponding element of $\mathrm{GF}(2^l)$ to the current symbol in the associated slice of the frame.

This channel model is then similar to an F-adder channel [44], with the difference that collisions may or may not occur and that, when collisions take place, the decoder can detect them.[16]

The upper bound (23) may now be derived as a simple consequence of the Rouché-Capelli Theorem. Regarding the information segments of the active users as the unknowns of a linear system of equations[17] and the symbol in $\mathrm{GF}(2^l)$ available in a non-empty slice as the known term of the corresponding equation, the system admits no unique solution whenever the number of unknowns exceeds the number of available equations. As $M \to \infty$ the expected fraction of non-empty slices is $1-\Psi_0 = 1-\exp\{-G/R\}$, while the expected number of unknowns per slice is equal to the expected channel load G which yields

$$G \leq 1 - e^{-G/R}$$

as a necessary condition for successful decoding. This inequality is equivalent to (27), the proof remaining the same hereafter.

It is pointed out that a similar proof technique was adopted in [20, Section II-D] to upper bound the success probability of the frameless scheme there considered. As it was recognized in [20], the bound there obtained represents a special instance of the capacity bound presented in this paper.

[16]It is worth pointing out that this simplified setting also represents a possible channel model for *shared memories*, provided some mechanism is employed to discriminate between memory locations in which the data of a single users are stored and memory locations in which the data of several users are XORed.

[17]Recall, in fact, that each encoded segment may be expressed as a linear combination of the associated information segments.

Acknowledgment

The authors would like to thank the Anonymous Reviewers and the Associate Editor for their insightful technical comments which helped to improve the paper.

References

[1] N. Abramson, "The ALOHA system – Another alternative for computer communications," in *Proc. 1970 Fall Joint Computer Conf.*, vol. 37. AFIPS Press, 1970, pp. 281–285.

[2] L. G. Roberts, "ALOHA packet systems with and without slots and capture," *ARPANET System Note 8 (NIC11290)*, Jun. 1972.

[3] N. Abramson, "Multiple access in wireless digital networks," *Proc. IEEE*, vol. 82, no. 9, pp. 1360–1370, Sep. 1994.

[4] D. Bertsekas and R. G. Gallager, *Data Networks*. Upper Saddle River, NJ, USA: Prentice-Hall, Inc., 1987.

[5] C. Morlet, A. B. Alamanac, G. Gallinaro, L. Erup, P. Takats, and A. Ginesi, "Introduction of mobility aspects for DVB-S2/RCS broadband systems," *IOS Space Commun.*, vol. 21, no. 1-2, pp. 5–17, Dec. 2007.

[6] W. Szpankowski, "Stability conditions for some multiqueue distributed systems: Buffered random access systems," *Adv. Appl. Probab.*, vol. 26, pp. 498–515, 1994.

[7] A. Ephremides and B. Hajek, "Information theory and communication networks: An unconsummated union," *IEEE Trans. Inf. Theory*, vol. 44, no. 6, pp. 2416–2434, Oct. 1998.

[8] R. R. Rao and A. Ephremides, "On the stability of interacting queues in a multiple access system," *IEEE Trans. Inf. Theory*, vol. 34, no. 5, pp. 918–930, Sep. 1988.

[9] J. Luo and A. Ephremides, "On the throughput, capacity, and stability regions of random multiple access," *IEEE Trans. Inf. Theory*, vol. 52, no. 6, pp. 2593–2607, Jun. 2006.

[10] A. Fanous and A. Ephremides, "Stable throughput in a cognitive wireless network," *IEEE J. Sel. Areas Commun.*, vol. 31, no. 3, pp. 523–533, Mar. 2013.

[11] E. Casini, R. De Gaudenzi, and O. del Rio Herrero, "Contention resolution diversity slotted ALOHA (CRDSA): An enhanced random access scheme for satellite access packet networks." *IEEE Trans. Wireless Commun.*, vol. 6, no. 4, pp. 1408–1419, Apr. 2007.

[12] G. L. Choudhury and S. S. Rappaport, "Diversity ALOHA – A random access scheme for satellite communications," *IEEE Trans. Commun.*, vol. 31, no. 3, pp. 450–457, Mar. 1983.

[13] Y. Yu and G. B. Giannakis, "High-throughput random access using successive interference cancellation in a tree algorithm," *IEEE Trans. Inf. Theory*, vol. 53, no. 12, pp. 4628–4639, Dec. 2007.

[14] S. Gollakota and D. Katabi, "Zigzag decoding: combating hidden terminals in wireless networks," in *Proc. ACM SIGCOMM 2008 Conf. Data Commun.*, ser. SIGCOMM'08, Seattle, WA, USA, 2008, pp. 159–170.

[15] J. L. Massey, *Collision-Resolution Algorithms and Random-Access Communications*, ser. Multiuser Communication Systems (CISM Course Lecture Notes), G. Longo, Ed. New York: Springer-Verlag, 1981, vol. 265.

[16] G. Liva, "Graph-based analysis and optimization of contention resolution diversity slotted ALOHA," *IEEE Trans. Commun.*, vol. 59, no. 2, pp. 477–487, Feb. 2011.

[17] A. Tehrani, A. Dimakis, and M. Neely, "Sigsag: Iterative detection through soft message-passing," *IEEE Trans. Signal Process.*, vol. 5, no. 8, pp. 1512–1523, Dec. 2011.

[18] T. Richardson and R. Urbanke, "The capacity of low-density parity-check codes under message-passing decoding," *IEEE Trans. Inf. Theory*, vol. 47, no. 2, pp. 599–618, Feb. 2001.

[19] F. Kschischang, B. Frey, and H.-A. Loeliger, "Factor graphs and the sum-product algorithm," *IEEE Trans. Inf. Theory*, vol. 47, no. 2, pp. 498–519, Feb. 2001.

[20] C. Stefanović, P. Popovski, and D. Vukobratovic, "Frameless ALOHA protocol for wireless networks," *IEEE Commun. Lett.*, vol. 16, no. 12, pp. 2087–2090, Dec. 2012.

[21] C. Stefanović and P. Popovski, "ALOHA random access that operates as a rateless code," *IEEE Trans. Commun.*, to appear.

[22] K. Narayanan and H. Pfister, "Iterative collision resolution for slotted ALOHA: An optimal uncoordinated transmission policy," in *Proc. the 7th Int. Symp. Turbo Codes and Iterative Inf. Process.*, Gothenburg, Sweden, Aug. 2012, pp. 136–139.

[23] C. Kissling, "Performance enhancements for asynchronous random access protocols over satellite," in *Proc. 2011 IEEE Int. Conf. Commun.*, Kyoto, Japan, Jun. 2011.

[24] Z. Shi and C. Schlegel, "Iterative multiuser detection and error control code decoding in random CDMA," *IEEE Trans. Signal Process.*, vol. 54, no. 5, pp. 1886–1895, May 2006.

[25] J. L. Massey and P. Mathys, "The collision channel without feedback," *IEEE Trans. Inf. Theory*, vol. 31, no. 2, pp. 192–204, Mar. 1985.

[26] J. Y. N. Hui, "Multiple accessing for the collision channel without feedback," *IEEE Trans. Veh. Technol.*, vol. 33, no. 3, pp. 191–198, Aug. 1984.

[27] G. Thomas, "Capacity of the wireless packet collision channel without feedback," *IEEE Trans. Inf. Theory*, vol. 46, no. 3, pp. 1141–1144, May 2000.

[28] S. Tinguely, M. Rezaeian, and A. J. Grant, "The collision channel with recovery," *IEEE Trans. Inf. Theory*, vol. 51, no. 10, pp. 3631–3638, Oct. 2005.

[29] S. Verdú, *Multiuser Detection*. Cambridge, U.K.: Cambridge University Press, 1998.

[30] K. W. Shum, C. S. Chen, C. W. Sung, and W. S. Wong, "Shift-invariant protocol sequences for the collision channel without feedback," *IEEE Trans. Inf. Theory*, vol. 55, no. 7, pp. 3312–3322, Jul. 2009.

[31] E. Paolini, M. Fossorier, and M. Chiani, "Generalized and doubly-generalized LDPC codes with random component codes for the binary erasure channel," *IEEE Trans. Inf. Theory*, vol. 56, no. 4, pp. 1651–1672, Apr. 2010.

[32] T. Helleseth, T. Kløve, and V. I. Levenshtein, "On the information function of an error-correcting code," *IEEE Trans. Inf. Theory*, vol. 43, pp. 549–557, Mar. 1997.

[33] A. Ashikhmin, G. Kramer, and S. ten Brink, "Extrinsic information transfer functions: Model and erasure channel properties," *IEEE Trans. Inf. Theory*, vol. 50, no. 11, pp. 2657–2673, Nov. 2004.

[34] E. Paolini, M. Fossorier, and M. Chiani, "Doubly-generalized LDPC codes: Stability bound over the BEC," *IEEE Trans. Inf. Theory*, vol. 55, no. 3, pp. 1027–1046, Mar. 2009.

[35] M. Ivanov, F. Brännström, A. G. i Amat, and P. Popovski, "Error floor analysis of coded slotted ALOHA over packet erasure channels," *IEEE Commun. Lett.*, vol. 19, no. 3, pp. 419–422, Mar. 2015.

[36] M. Shokrollahi, *Capacity-Achieving Sequences*. Minneapolis, USA: Inst. Mathematics and its Applications (IMA), vol. 123, IMA Volumes in Mathematics and its Applications, pp. 153–166, 2000.

[37] K. Price, R. Storn, and J. Lampinen, *Differential Evolution: A Practical Approach to Global Optimization*. Berlin, Germany: Springer-Verlag, 2005.

[38] S. Kudekar, T. Richardson, and R. Urbanke, "Threshold saturation via spatial coupling: Why convolutional LDPC ensembles perform so well over the BEC," *IEEE Trans. Inf. Theory*, vol. 57, no. 2, pp. 803–834, Feb. 2011.

[39] G. Liva, E. Paolini, M. Lentmaier, and M. Chiani, "Spatially-coupled random access on graphs," in *Proc. 2012 IEEE Int. Symp. Inf. Theory*, Cambridge, MA, USA, Jul. 2012, pp. 478–482.

[40] A. Munari, M. Heindlmaier, G. Liva, and M. Berioli, "The throughput of slotted Aloha with diversity," in *Proc. the 51st Annual Allerton Conf. Commun., Control, and Computing*, Monticello, IL, USA, Oct. 2013.

[41] O. del Rio Herrero and R. De Gaudenzi, "A high-performance MAC protocol for consumer broadband satellite systems," in *Proc. the 27th AIAA Int. Commun. Satellite Syst. Conf.*, Edinburgh, UK, Jun. 2009.

[42] M. Ghanbarinejad and C. Schlegel, "Irregular repetition slotted ALOHA with multiuser detection," in *Proc. the 10th Annual Conf. Wireless On-demand Netw. Syst. Services*, Banff, AB, Mar. 2013, pp. 201–205.

[43] G. Liva, E. Paolini, B. Matuz, S. Scalise, and M. Chiani, "Short turbo codes over high order fields," *IEEE Trans. Commun.*, vol. 61, no. 6, pp. 2201–2211, Jun. 2013.

[44] R. Urbanke and B. Rimoldi, "Coding for the F-adder channel: Two applications of Reed Solomon codes," in *Proc. 1993 IEEE Int. Symp. Inf. Theory*, San Antonio, TX, USA, Jan. 1993, p. 85.

Enrico Paolini (M'08) was born in Fano, Italy, in 1977. He received the Dr. Ing. degree (summa cum laude) in Telecommunications Engineering in 2003 and the Ph.D. degree in Electrical Engineering in 2007, both from the University of Bologna, Italy.

While working toward the Ph.D. degree, he was Visiting Research Scholar with the Department of Electrical Engineering of the University of Hawai'i at Manoa, Honolulu, HI. Currently, he is an Assistant Professor at the Department of Electrical, Electronic, and Information Engineering "Guglielmo Marconi", University of Bologna. His research interests include error-control coding, random access techniques with successive interference cancellation, and tracking algorithms in radar systems. In the field of error correcting codes, he has been involved since 2004 in several activities with the European Space Agency. He is a frequent visitor at the Institute of Communications and Navigation of the German Aerospace Center, where he was Visiting Scientist in 2012 and 2014 under DLR-DAAD fellowships.

Dr. Paolini is Editor (of iterative decoding methods and fountain coding) for the IEEE TRANSACTIONS ON COMMUNICATIONS and past Editor (2012–2015) for the IEEE COMMUNICATIONS LETTERS. He served on the Technical Program Committee at several IEEE International Conferences. He also served on the Organizing Committee (as co-chair) of the ICC'14 and ICC'15 Workshop on Massive Uncoordinated Access Protocols (MASSAP).

Gianluigi Liva (M'08–SM'14) was born in Spilimbergo, Italy, in 1977. He received the M.S. and the Ph.D. degrees in electrical engineering from the University of Bologna (Italy) in 2002 and 2006, respectively.

Since 2003 he has been investigating channel codes for high data rate CCSDS (Consultative Committee for Space Data Systems) missions. From October 2004 to April 2005 he was researching at the University of Arizona in Tucson, where he was designing low-complexity error correcting codes for space communications. Since 2006 he is with the Institute of Communications and Navigation at the German Aerospace Center (DLR), where he currently leads the Information Transmission group. In 2010 he has been appointed lecturer for channel coding at the Institute for Communications Engineering (LNT), Technische Universität München (TUM). In 2012 and 2013 he has been lecturing for channel coding at the Nanjing University of Science and Technology (China). Since 2014 he is lecturer for channel codes with iterative decoding at the Institute for Communications Engineering (LNT), Technische Universität München (TUM). His main research interests include satellite communications, random access techniques and error control coding. He is/has been active in the DVB-SH, DVB-RCS and DVB-S2 standardization groups, as well as in the standardization of error correcting codes for deep-space communications within the CCSDS.

He received the 2007 IST Mobile & Wireless Communication Summit Best Paper Award. He has been co-chair of the First DLR Workshop on Random Access and Coding (2013), of the 2014 Sino-German Workshop "Bridging Theory and Practice in Wireless Communications and Networking" in Shenzhen (China), of the IEEE ICC 2014 Workshop on Massive Uncoordinated Access Protocols (MASSAP) in Sydney (Australia) and of the 2015 Munich Workshop on Coding and Modulation.

Marco Chiani (M'94–SM'02–F'11) received the Dr. Ing. degree (summa cum laude) in electronic engineering and the Ph.D. degree in electronic and computer engineering from the University of Bologna, Italy, in 1989 and 1993, respectively.

He is a Full Professor in Telecommunications at the University of Bologna. During summer 2001, he was a Visiting Scientist at AT&T Research Laboratories, Middletown, NJ. Since 2003 he has been a frequent visitor at the Massachusetts Institute of Technology (MIT), Cambridge, where he presently holds a Research Affiliate appointment. He is leading the research unit of the University of Bologna on cognitive radio and UWB (European project EUWB), on Joint Source and Channel Coding for wireless video (European projects Phoenix-FP6, Optimix-FP7, Concerto-FP7), and is a consultant to the European Space Agency (ESA-ESOC) for the design and evaluation of error correcting codes based on LDPCC for space CCSDS applications. His research interests are in the areas of wireless systems and communications theory, including MIMO statistical analysis, codes on graphs, wireless multimedia, cognitive radio techniques, and ultra-wideband radios.

He received the 2011 IEEE Communications Society Leonard G. Abraham Prize in the Field of Communications Systems, the 2012 IEEE Communications Society Fred W. Ellersick Prize, and the 2012 IEEE Communications Society Stephen O. Rice Prize in the Field of Communications Theory. He is the past chair (2002–2004) of the Radio Communications Committee of the IEEE Communication Society and past Editor of Wireless Communication (2000–2007) for the journal IEEE TRANSACTIONS ON COMMUNICATIONS. In 2012 he has been appointed Distinguished Visiting Fellow of the Royal Academy of Engineering, UK.